Politecnico di Milano

SCHOOL OF INDUSTRIAL AND INFORMATION ENGINEERING

Master of Science – Energy Engineering

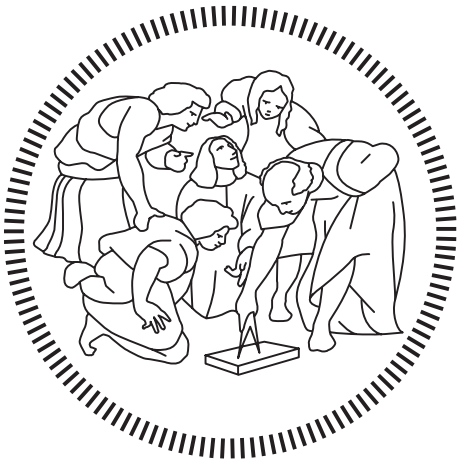

Simulation of Coupling a Solar Thermal System with Ground Source Heat Pump for a Single House in Cold Weather with TRNSYS

Supervisor

Prof. Luca MOLINAROLI

Co-Supervisor

Prof. Marilyn LIGHTSOTNE

Candidate

Mohammad ZAMANIAN – 894017

Academic Year 2019 – 2020

Acknowledgements

I would like to express my immense gratitude and sincerity towards Prof. Molinaroli, my supervisor and Professor of Politecnico di Milano for his unfailing support and help during this project. It could not be possible to finish this work without his great ideas in this project, which I took advantage of at most.

I would also like to acknowledge Prof. Lightstone, my second supervisor and Professor of McMaster University in Canada, who provided me this opportunity to come to Canada and supported me with her valuable comments on this project. Not only I learned so much from her in this field of engineering, but also I learned a lot from her extra-ordinary pleasant personality.

Lastly, I should express my gratitude to my parents who have always been my first supporters and have been encouraging me throughout the years of my studying and whole life. No words can describe my gratitude towards them. My accomplishment wouldn't have been possible without the support and love of all of these great people

Abstract

Ground source heat pump system extracts energy from the ground via a borehole heat exchanger. The borehole heat exchanger is created by drilling a very long borehole (can be 100-300 m long) with a diameter of roughly 6-8 inches. A tube (doubled over so that it forms a "U") is placed into the ground and surrounded by a grout that provides good heat transfer between the tube and the adjacent soil. A heat transfer fluid (water or water/glycol mixture) flows through the tube line and exchanges heat with the ground. In the winter time, energy is extracted from the ground and used for household space heating. While in the summer (when the air conditioner is used), energy is extracted from a house and deposited in the ground.

The challenge we face is that in heating-dominated climates, such as Canada, more energy is extracted from the ground in the winter than is replenished in the summer. The outcome of this is that the soil will cool down over time, resulting in lower values of the heat pump coefficient of performance, and the overall system performance will decline.

We will investigate the idea for solving this problem in this study relying on solar domestic hot water systems, which use solar thermal collectors to heat water for domestic use. These systems are relatively simple: collectors, piping, pump, hot water tank, and controllers. The collector area is sized to provide high solar fractions in the summer; however, the solar fraction in the winter is low. In Toronto, annual solar fractions (defined as energy from solar thermal system/total energy needed by the load) are around 50-60%. This work aims to use the solar thermal collector to recharge the ground in the summer. This would allow for larger collector areas, and thus better performance in the winter, and the excess energy in the summertime would be deposited in the ground. The current study has been conducted for a single house, so talking about the solar thermal collector area and being large should be around 5 m^2. This would help with balancing the seasonal heat transfer to the ground, which could alleviate the long-term drop in performance that can occur with ground source heat

pumps. The study shows that coupling the solar thermal system with the ground source heat pump would meet our target. Using this system, the temperature of the ground, whose initial temperature is 14 °C, would increase by 24% (from 10.88 °C to 13.49 °C) for a borehole heat exchanger length of 150 m in Toronto, ON, Canada.

Keywords

Ground Source Heat Pump (GSHP), Borehole Heat Exchanger, Heat Transfer, Solar Fraction, Solar Thermal Collector, Thermal Imbalance

Table of Contents

List of Figures

List of Tables

Chapter 1
Introduction

1.1 Background

Fossil fuels have been and continue to be a predominant energy source across the globe since the industrial revolution. In 2017, fossil fuels represented 81% and 76% of the total worldwide and Canadian prime energy supply, respectively [22]. In the past decades, fossil fuel consumption has raised concerns due to its detrimental impacts on the global environment. The alarming increase in greenhouse gas emissions levels and the political tensions associated with fossil fuels are contrary to sustainable development. They are the main driving forces to seek alternative renewable energy to lift dependence on fossil fuels. As a member of the G7, Canada pledged to phase out fossil fuels and reformed fiscal support for oil and gas production to seek a low carbon economy [23]. Renewable resources like solar, wind, tidal, and biomass offer great potentials to meet the requirements of sustainable development with a low carbon economy, and solar energy is the most abundant among those above. In Canada, 17% of the total energy produced is consumed by households, and 82% of this amount is utilized for space and water heating [24]. Solar thermal systems are promising applications to offset the dependence on fossil fuels for domestic heating demands. The solar collector captures and converts solar energy into thermal energy to fulfill household needs. A successful precedent near Calgary, Alberta, is the Drake Landing Solar Community (DLSC), where more than 90% of the residential space heating demand was fulfilled by solar energy spanning over the years 2012- 2016 [25]. During the summer season, solar energy was harnessed and converted into thermal energy. The energy that was not immediately needed was stored underground using the borehole thermal energy storage, where it could be accessed during the wintertime when solar irradiance is not found in abundance. It showed a reduction of approximately five tons of annual greenhouse gas

emissions per home. This demonstrated the great benefit of solar thermal systems for sustainable development and low carbon economy. Although Ontario does not receive as much solar irradiance as Alberta, as shown in Figure 1-1 [28], solar water heating systems potentially can offer a significant reduction in nonrenewable energy consumption in single house applications. For instance, a Solar Domestic Hot Water (SDHW) system can provide 50% of hot water, which is needed for a four-person household, and reduce up to two tons of CO2 emissions annually [26].

Numerical simulations are cost-effective, time-efficient, and allow for quick adjustment of system parameters. In this thesis, the commercial system simulation computer code TRNSYS 18 [27] is used to study system performance under a specific operating condition.

In light of this, we decided to use a green energy source system to provide the demands of a single house in Canada to meet the G7 agreement on reducing CO_2. This green energy source is coming from both the sun and the earth to provide hot water and store the energy.

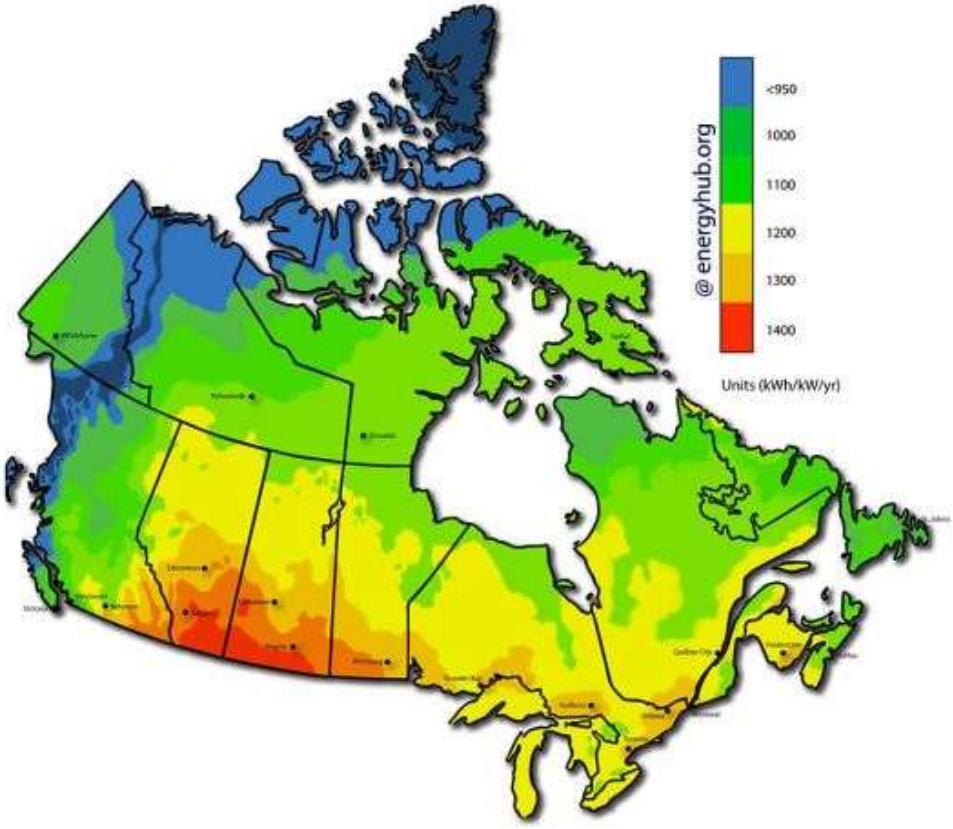

Figure 1-1 Solar irradiance map for Canada [28]

1.2 Objective and Strategy

The purpose of this work is to numerically investigate the role of the solar thermal collector in providing hot water for domestic usage and the necessary energy to be stored in the ground due to the thermal decline of the soil temperature in winter.

The commercial software, TRNSYS (version18), will be used to simulate the system behaviors. TRNSYS uses the Finite Difference Method (FDM) to solve a series of differential equations which describe the entire system. The results will be supported by the completion of the components and the system components independently. Subsequently, thermal behaviors of the system, such as soil temperature, hot water temperature, to name but a few, will be investigated at specific mass flow rates in the collector, load side, and in the ground source heat pump.

1.3 Thesis Outline

This thesis is divided into four different chapters, including introduction, literature review, system identification, and results and discussion.

Literature review (chapter 2) is a concise review on the most valuable projects and works which have been done on the Solar Domestic Hot Water (SDHW), Ground Source Heat Pump (GSHP), and Combined Solar Collector-Geothermal Heat Pump (CSCGHP) Systems, discussing the system performance, thermal stratification specifically in storage tanks, classification of different components and elements, temperature distribution on different parts of the model, few to mention.

System identification (chapter 3) describes the most essential components and their performances in our model, including solar collector, storage tanks, borehole heat exchanger, and heat pump.

Results and discussion (chapter 4) explores our targets in this work, with more weight on the temperature distribution of the house, soil, hot water, and other parameters. It also shows the

results in figures and shapes. Finally, we will discuss other possible works which could be done on this subject of engineering as a proposal.

Chapter 2
Literature Review

Solar thermal collectors, storage tanks, borehole heat exchangers, and heat pumps play a significant role in the Solar Domestic Hot Water System Coupled with Ground Source Heat Pump (SDHWSCGSHP) systems. In this chapter, we will summarize some the most important studies done on this kind of system and related to our project.

2.1 Literature Review

A computer simulation was conducted in TRNSYS by Kjellsson et al. [1] aimed to analyze different systems in which solar thermal collectors and ground source heat pumps are connected. In their study, large differences were found between the system alternatives. Also, the optimal design in this simulation was when solar heat produces domestic hot water during summertime and recharges the borehole in the winter. They proved that the advantage is, among other factors, because of the heat extraction rate from the borehole and the overall design parameters of the system. This study demonstrates that the electricity demand may increase with solar recharging due to the increased operating time of the circulation pumps. Moreover, other port of the results shows that another advantage with solar heat combined with heat pumps is when the boreholes or neighboring installations are drilled so close to each other so that they influence each other thermally. This may decrease temperatures in the ground, which gives a decreased performance of the heat pump and increased electricity use.

Chargui and Sammouda [2] propose a heating a residential house using the abundant and universal sources for a residential house in Tunisia. And they have studied the

omnidirectional impact of incidence solar radiation in a heat pump mounted in a residential complex during winter. This team presented a mathematical description of the house in TRNSYS along with the results of the numerical study of several components. Also, their study attempts to measure the temperature distribution, the incidence solar radiation, as well as the delivered and consumed energy, and its impact on air-conditioning load in rooms using the Tunisian climate. Numerical results of this research have been obtained for 24 hours in January and 4500 hours operation in the winter. Additionally, results show that the system may be satisfactorily used for residential building or greenhouse heating in the Mediterranean and region of Tunisia.

Mehrpooya et al. [3] made an investigation on optimization of performance of Combined Solar Collector-Geothermal Heat Pump (CSCGHP) Systems to supply thermal load demanded for heating greenhouses. Their main purpose was to analyze the system from technical and economical standpoints. To optimize the technical aspect of the system, the operation of the controllers, diverters and mixers was changed with several control algorithms to preheat the fluid going into the heat pump evaporator. The regulation of this temperature up to an ideal value was done successfully, resulting in an increase in ground heat recovery during maximum heat extraction intervals, maximal gorund source heat exchanger outlet temperature, and the performance coefficient of the heat pump. It also led to a decrease in the required minimum auxiliary energy for heating the greenhouse and heat recovery during summer season. Furthermore, aiming at balancing between economical and technical issues in this study, from economical point of view the optimum condition was calculated and the corresponding final optimized design was determined. The selected model in this research has an average seasonal coefficient of performance equal to 4.14, a borehole length equal to 50 m, and number of boreholes equal to 3. Moreover, total collector area of the model in this research is 9.42 m^2. Finally, a comparison between the final optimized system with an exchanger using the best working fluid for each loop and the same system with one single fluid was done in the published paper of this research.

A GSHP system used for space heating in a cold climate was investigated in Emmi et al. [4] study. In this research, the solar-assisted ground source heat pump extracted heat from the ground using borehole heat exchangers and then injected excess solar thermal energy into the ground. Their model was simulated based on the heating mode in cold climates regarding the building load profiles. However, when common ground source heat pump systems are

used only for heating, their performance drops due to an unbalanced ground load. Emmi et al. implemented their simulation in TRNSYS performed in six cold locations to investigate solar-assisted ground source heat pumps. The borehole length effect was analyzed, particularly in terms of the energy efficiency of the heat pump. Finally, a suitable control strategy was utilized to manage both the solar thermal collectors and the borehole heat exchangers.

In another research Chen and Yang [5] presented the numerical simulation of a solar assisted ground coupled heat pump (SAGCHP) system which can supply both domestic hot water and space heating. In their study the optimization process was accomplished on TRNSYS by simulating the effect of solar collector area on the total borehole length and system performance. Their simulations were also done under different meteorological weather conditions to explore the applicability of the proposed SAGCHP system in northern China. The simulated results of their study demonstrated that a collector area of 40 m^2 and a borehole length of 264 m are optimized system parameters under the specified load conditions. The annual total heat extraction added by 75% of the hot water requirement can be provided by solar energy in the optimized design. Moreover, the optimized design energy balance was validated with a minor error margin of 0.75%, and the system proved to have more efficiency and economic incentives for its application in Beijing area.

The main objective of Ozgener's study [6] was to investigate the performance characteristics of a SAGSHPGHS with a vertical 50 m and a nominal diameter of 1 × 1/4 in U-bend ground heat exchanger via exergy analysis. This model was implemented in Solar Energy Institute of Ege University, Izmir, Turkey. In this research exergetic efficacy of the system components were determined in an attempt to assess their performances. 2.64 and 2.38 are the results of this work for the coefficient of performances of heating of the ground-source heat pump unit and the whole system, respectively, while the exergetic efficiency of the overall system obtained to be 67.7%.

In other study carried out by Rad et al. [7], overall system feasibility of a SAGSHP system was evaluated for cold climates using a dynamic system simulation approach. The shortcoming of the SAGSHP system for an actual house, and the solutions to tackle these deficiencies were successfully addressed through implementing the modelling and simulation of the installed SAGSHP system. The results of this work showed that the hybrid

ground source heat pump system with solar thermal collectors is a feasible choice for space heating of a house in cold climate. This study also demonstrated the value in utilizing a system simulation approach to evaluate alternatives in complex systems.

The performance of a ground source heat pump (GSHP) system with horizontal coupled ground loop pipes was monitored, analyzed, extrapolated and numerically simulated in the Safa and co-worker's study [8]. Their research was aimed to develop cooling or heating performance curves based on the building loads and the source temperatures. They also evaluated the heat pump efficiency at different load/source temperatures, and measured the compressor cycling characteristics. Furthermore, the heat pump in this study was modeled adopting the performance curves obtained from the experimental investigation. In this research, the model was validated using the daily thermal output and determined the range of COP from 3.05 (at an ELT of 44.4 °C and an EST of 2.7 °C) to 3.44 (at an ELT of 41.5 °C and an EST of 5.48 °C). The system was also scrutinized for potential improvements in the control strategies.

Solar assisted ground-source heat pump (SAGSHP) heating apparatus with latent heat energy storage tank (LHEST) is investigated by Han et al. [9]. After developing a mathematical model for the system, a transient numerical simulation was conducted. The operation characteristic of the heating system in this study was analyzed during the heating period in Harbin. From the results of the simulation, the average coefficient of performance (COP) of the heating system was 3.28 in heating period. The system displayed a higher COP in both the initial and latter heating intervals with a maximum value of 5.95.

An analytical model was implemented to model the steady-state heat transfer in double U-tube boreholes sporting two independent circuits operating with dissimilar mass flow rates and inlet temperatures. The model which was presented by Eslaminejad and Bernier predicted the fluid temperature profiles in both circuits along the borehole depth [10]. The proposed model in this study was used to investigate a novel double U-tube borehole configuration with a single circuit linked to a ground-source heat pump operating in heating mode, and the other circuit to the thermal solar collectors. All systems in this study was simulated over a twenty-year period for a residential-type single-borehole configuration. Results of this research revealed that winter solar recharging, either for the proposed configuration or the solar assisted ground-source heat pump system, causes 194 and 168%

reduction in the amount of energy the heat pump extracts from the ground. It was also shown that, for a ground thermal conductivity of 1.5 W/m/K, the borehole length can be reduced by as much as 17.6%, and 33.1% in the case of using the proposed configuration or the solar assisted ground-source heat pump system. Also, the influence on the annual heat pump energy consumption was less dramatic, corresponding to 3.5% and 6.5% reduction.

Another research program at Brookhaven National Laboratory (BNL) has studied the use of the earth as a heat sink for solar-assisted heat-pump systems [11]. Part of this work is dedicated to four tanks that were buried into the ground to evaluate the probability of ground-coupled tanks for this application in a specific period, from December 1978 to March 1981. The energy in the form of heat was either injected into or rejected from the tanks on a weekly computer simulation of solar-assisted heat-pump systems in the local climate (in New York). Each tank was operated with a different control strategy. This study revealed experimental results from these tanks for the mentioned period and compared the experimental results to those obtained by a computer model, GROCS, developed at BNL. Its results showed a sensitivity to the soil thermal conductivity during periods of large heat addition to the tanks. A ground-coupled tank was found to be suitable in series solar-assisted heat-pump systems. However, no vital carry-over of summer-collected heat to winter was observed.

Emmi et al. [12] evaluated the thermal behavior of ground source heat pumps in cold climates, where the thermal load profile of buildings was not balanced in terms of heating and cooling, especially in the residential sector whose significant characteristic is low internal loads. In this context, the heat pump mainly works in heating mode, continuously extracting heat from the soil. Consequently, the ground temperature decreases gradually over the years affecting the energy performance of the heat pump. In this study a multi floors residential building with 12 flats (88 m^2 each) was analyzed in three climate zones, making use of the simulation tool TRNSYS. Different configurations of the plant system investigated thoroughly and the case without the solar thermal collectors has been considered as reference. Results of this research show that the ground is subject only to the extraction of heat for heating and the mean ground temperature therefore decreases during the years jeopardizing the heat pump performance. When solar thermal collectors are integrated, the total borehole length can be reduced, making the initial cost of installing the borehole more economic.

In another research done by Tian You et al. [13], a general overview of the main problems caused by soil thermal imbalance and their existing solutions is presented. The caused problems were mainly presented in their research in the following aspects: soil temperature decrease, heating performance deterioration, heating reliability decline, and even system failure. Also, there are couple of solutions presented in this study which are classified into thermal and physical properties of the borehole heat exchanger, including borehole spacing, borehole. By changing and improving these parameters, we can even out the thermal imbalance to some extent, suitable to projects with slight imbalance. The results in this study have been compared to the ones obtained in the current work.

In Cimmino and Eslami-Nejad's research [14], the required borehole heat exchanger length regarding different network arrangements was tested under variation of minimum fluid temperature returning to the heat pump, total solar collector area, and borehole spacing. All cases were compared against one borehole configuration, with and without injection of solar heat. Results of this study showed that as the injection of solar heat into the ground increases, the required borehole length decreases by a more significant amount for a field of shallow boreholes compared to a deep borehole configuration. Minimum fluid temperatures returning to the heat pump plays a significant role in the required borehole length for both a one borehole configuration and shallow borehole fields (50% and above, from 0 °C to -5 °C). For shallow borehole networks, borehole spacing must be determined carefully. The total required length of shallow borehole fields can be shorter, as a one borehole arrangement.

Several well-known models for the purpose of estimation of solar radiation components on horizontal and inclined surfaces were reviewed in Mousavi Maleki's research [15]. To find the best model for a given location the hourly outputs predicted by available models were compared with the field measurements of the given location. The main objective of this study was to review on the evaluation of the most accurate models for estimating solar radiation components for a given location, by testing various models. In this study, to increase the amount of incident solar radiation on photovoltaic (PV) panels, the PV panels were mounted on tilted surfaces. This research also provides an up-to-date status of different optimum tilt angles that have been determined in various countries.

To assess electrical load shifting in order to reduce peak electricity demand, a detailed numerical model for a ground-source heat pump connected to a thermal storage was developed by Teamah and Lightstone [16] for residential heating applications. In this research, water-based thermal storage and hybrid storage containing water and phase change materials (PCMs) were considered. The amount of thermal buffering needed to shift the heat pump operation to off peak electricity periods was numerically assessed for a house of 180 m^2 floor area in Toronto, Ontario, Canada. Results of this study indicated that total electrical load shift to off-peak hours was achieved by a 2.5 m^3 water tank or a 1 m^3 hybrid tank containing 50% PCM by volume. This implies an approximate 65% decrease in storage volume without affecting the space heating capability. Also, the influence of operating temperature ranges and the packing ratio was presented. Lower operating ranges and higher packing ratios result in better thermal buffering of the hybrid system at smaller storage volumes. However, careful choice of the PCM encapsulation geometry was needed to ensure total melting/solidification during the charging/discharging period.

Sommerfeldt and Madani conducted a parametric study of the technical performance and economic benefits of the ground source heat pump (GSHP) systems connected with a series of solar PV/thermal (PVT) collectors [17]. The focus of attention in this study was on the multi-family houses (MFH) in Sweden with a heating-dominant climate, where the heat pump market is restricted due to land deficiency for boreholes or noise limitations on air heat exchangers. System efficiency and lifecycle cost results were generated using a holistic and detailed systems model in TRNSYS over twenty years. The results showed that PVT could reduce borehole length by 18% or spacing by 50% while maintaining an identical seasonal performance factor. The PVT+GSHP system cost is higher than a traditional PV+GSHP system. However, this fact fails to account for the value of the land area saved by the PVT system, which can be up to 89%. Another result of this study disclosed that the reduction in land area due to using a PVT system could increase the use of GSHP in MFH and promote solar energy diffusion in high latitude markets.

Trillat-Berdal et al. [18] conducted an experimental study on a ground-connected heat pump in combination with thermal solar collectors. This configuration satisfies domestic hot water and heating–cooling needs. Solar heat was used as a priority for domestic hot water heating and when the preset water temperature was reached, excess solar energy was injected into the ground via boreholes. This system contributes to the balance of the ground loads,

increasing the operating time of the solar collectors and avoiding overheating problems. After eleven months of operating, the average amount of power extracted from and injected into the ground was equal to 40.3 and 39.5 W/m, respectively. The results of this study demonstrated that energy injected into the ground amounts to 34% of the heat extracted, and the heat pump coefficient of performance (COP) in heating mode was 3.75. In addition, the domestic hot water solar fraction had an average value higher than 60% for the first eleven months of operation.

Research, done by Wuestling et al. [19], presents the results of using the TRNSYS in which the thermal performance of solar domestic hot water (SDHW) facilities utilizing alternative control strategies operating under realistic conditions in several different climates of the United State was compared. Also, The effects on system performance based on the time of year, collector area and quality, preheat storage tank volume and energy losses, occurrence of mixing the preheat storage tank, controller temperature dead-bands, auxiliary set temperature, total daily usage, and load distribution were investigate in this research. Result also showed that for the particular reduced constant flow rate systems investigated, the annual performance with stratified storage at reduced flow rates showed an absolute improvement from 11.5 to 14.7 percentage points greater than that which would be achieved with fully mixed storage tanks operating at conventional collector flow rates.

In another research at the Jiangsu University of Science and Technology, Zhao et al. [20] compared conventional ground source heat pump system (GSHPS), and GSHPS with different heat recovery ratios, in a typical city, in terms of thermal imbalance ratios, average soil temperatures and soil temperature increases. In their study the transient system simulation software was used to simulate the operation performance of GSHPS. Result indicates that the thermal imbalance ratio and soil temperature decreased with increasing heat recovery ratio. Also, after a twenty-year operation, the ratios of soil thermal imbalance in the GSHPS were 29.2%, 21.1%, 16%, and 5.2%, and the increase in soil temperature equaled 8.78, 5.25, 3.44, and 0.34 °C, respectively. At the same time, the heat recovery ratios were 0, 18%, 30% and 53%, correspondingly. It was finally concluded that a GSHPS with heat recovery is potentially efficient and affordable for buildings in regions with hot summers and cold winters.

A ground heat pump system coupled with a solar thermal storage unit was shown to solve the performance degradation problem caused by the drop in the soil temperature in a study conducted by Nam et al. [21]. In addition, the system performance was analyzed and compared under difficult heating conditions using TRNSYS. Results of this study demonstrated that the ground heat pump system in tandem with solar thermal can effectively maintain the soil temperature balance and during the entire operation time, the heat exchange rate and heat pump COP of solar-assisted ground heat pump system (SAGHPS) were 43.3 and 4.7 W/m. Compared with GSHPS, the above parameters saw an increase of 28.1% and 9.3%, respectively. Also, the increase in collector area and the upgraded heating performance of the system led to a relative rise in investment costs. The results of the LCC assessment indicated that when the solar collector area increased from 50 m^2 to 90 m^2, the payback period of SAGHPS would be in the range of ten to twelve years.

2.2 Conclusion

This chapter summarized some of the important projects and works done on SDHW, GSHP, and CSCGHP Systems and described their results. In light of these works, we inspired our topic to work on the SDHWSCGSHP system for a single house in a heating-dominant place, i.e. in a location with cold climate such as Toronto City in Ontario, Canada, to improve the thermal imbalances in the ground while the system simultaneously produces the hot water for the domestic demands. In the next chapter, we will discuss different components and their performances in our model used in TRNSYS.

Chapter 3
System Identification

This chapter describes the main components that have an important role in our model, including their performance, governing equations, and how they perform in TRNSYS. As it's described before, TRNSYS is a commercial simulation software which connects a series of different components to predict the behaviors of a transient system, such as SDHW, GSHP systems, to name but a few. TRNSYS employs an FDM to solve differential equations that describe the entire system. This chapter is divided into three sections. Each section will be dedicated to one of the essential components, including the solar thermal collector, storage tank, and borehole heat exchanger connected with the heat pump.

3.1 Solar Thermal Collector

The flat-plate solar collector, Type 1b, is investigated in this section. This component models the thermal performance of a flat-plate solar collector including the outlet temperature of the solar collector and useful energy gain by applying the Hottel-Whillier equation [27, 30]. The solar collector array may consist of collectors connected in series and parallel. In our model, a single flat-plate solar collector whose parameters are reported in Table 3-1 is used. The governing equation on this type of solar collector is the one that Hottel-Whillier expressed as a relation between the energy collected by the collector, collector properties, and weather data, Equation 3-1.

$$Q_u = A_C\,[F_R(\tau\alpha)G_T - F_R U_L(T_i - T_a)] \qquad \text{Equation 3-1}$$

A general equation for solar thermal collector efficiency can be also obtained from the Hottel-Whillier equation as follows, Equation 3-2:

$$\eta = \frac{Q_u}{A_C G_T} = F_R(\tau\alpha) - F_R U_L \frac{(T_i - T_a)}{G_T} \qquad \text{Equation 3-2}$$

The model for Type 1b is conducted on a summer day (August 31) and a winter day (February 1). The fluid which is running through the system (solar collector) is Ethylene Glycol, which is a clear, sweet, slightly viscous liquid. A 60 percent solution of ethylene glycol and water boils at 111.1 °C (232 °F) and freezes at −52.8 °C (−63 °F), serving as an excellent solution for solar collector systems in extremely cold weather. Ethylene glycol is highly poisonous; animals or humans that drink the solution become very ill and may die [29]. Other physical properties of this substance is reported in Table 3-2. Also, the typical meteorological weather data used in the model is extracted from the TRNSYS database for Toronto, ON, Canada [27].

The simulation results are plotted in Figure 3-1 and Figure 3-2 for T_o and Q_u, respectively. It indicates that TRNSYS predicts the results in align with the governing equations described above.

Table 3-1 Solar Collector Parameters

Description	Value	Units
Number in series	1	-
Collector area ($\boldsymbol{A_C}$)	5	m^2
Fluid specific heat ($\boldsymbol{C_p}$)	3.284	kj/kg/K
Tested flow rate ($\dot{m}_f$)	40	$kg/hr/m^2$
Intercept efficiency ($\boldsymbol{F_R(\tau\alpha)}$)	0.80	-
Efficiency slope ($\boldsymbol{F_R U_L}$)	13	$kj/hr/m^2/K$
Efficiency curvature	0.05	$kj/hr/m^2/K^2$
Initial temperature	20	℃

Table 3-2 Ethylene Glycol Solution (60%) Physical Properties at 20 °C

Description	Value	Units
Density	1095	kg/m^3
Specific Heat	3.284	kj/kg/K

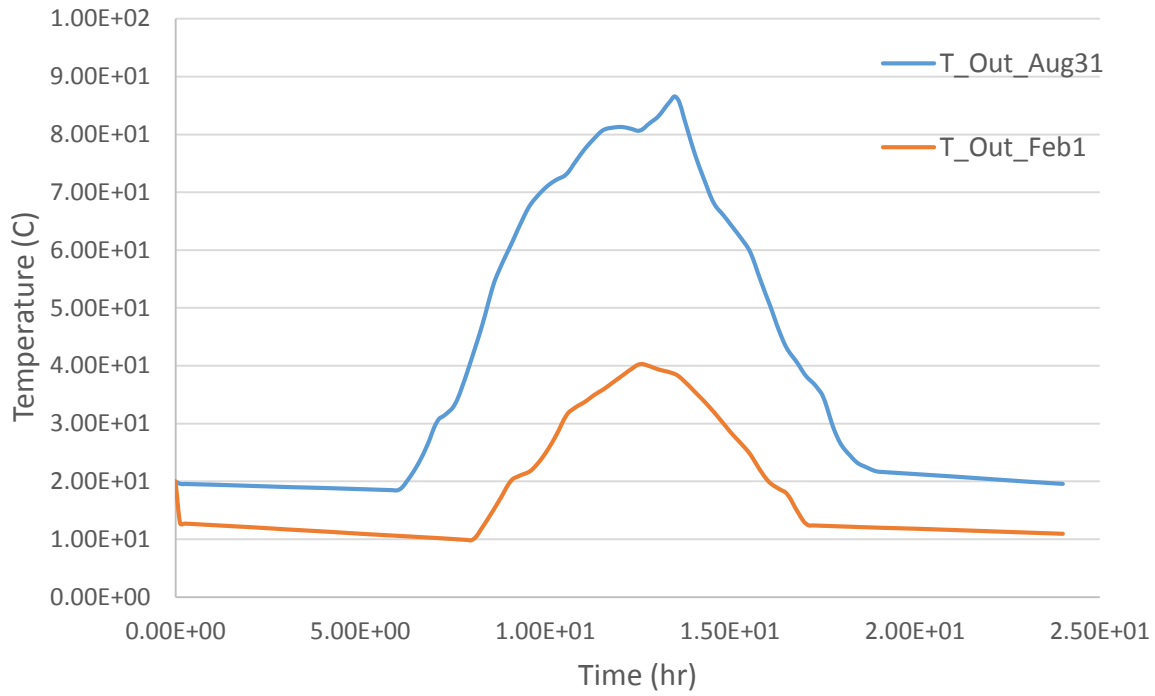

Figure 3-1 TRNSYS Results for Solar Collector Outlet Temperature versus Time in Toronto, ON, Canada

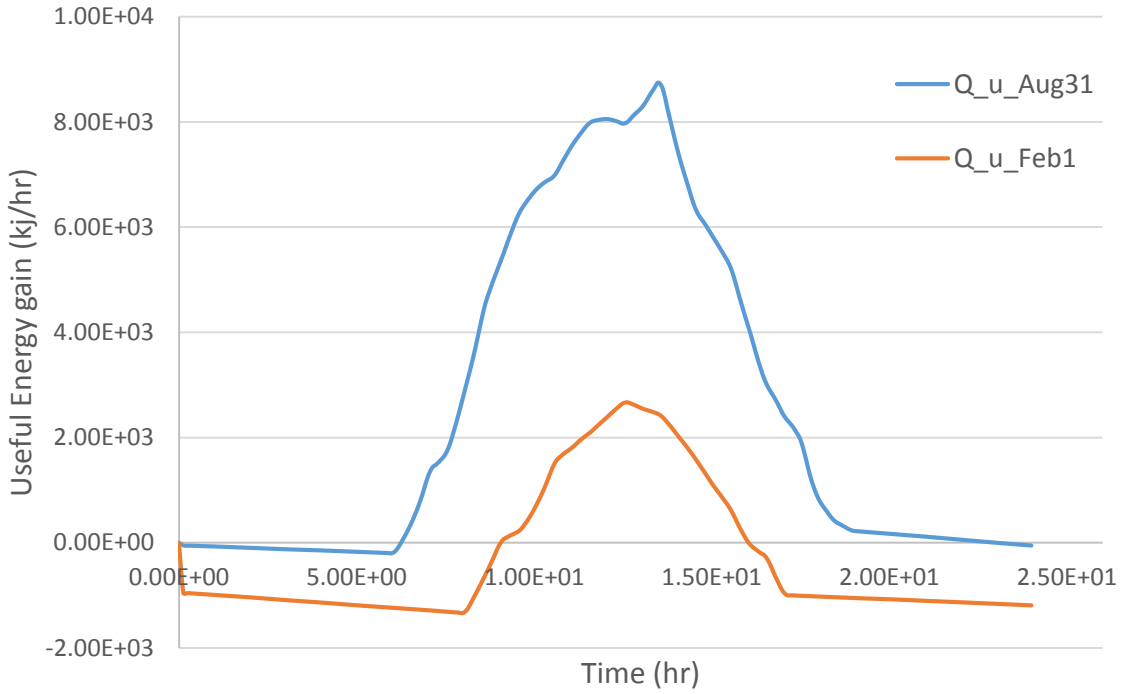

Figure 3-2 TRNSYS Results for Useful Energy Gain versus Time in Toronto, ON, Canada

3.2 Storage Tank

TRNSYS supports a significant number of tank models. These tanks are classified as Nodal and Algebraic tanks, depend on the method of specifying the size of a node (grid spacing). By solving the one-dimensional transient thermal energy equations, we can get the temperature distribution within the tank, which is influenced by heat transfer between different parts of the tank, including convection by the fluid, axial heat conduction, and losses through the walls [27].

An algebraic tank determines the temperature profile of a stratified tank by using the size segments of the fluid, which depends on the magnitude of the flow rate, the magnitude of the simulation time-step, and the magnitude of the heat losses at both the charging and discharging mode. The advantage of these tanks over the nodal ones is that they can model the temperature stratification based on a small temperature gradient zone within the grid; therefore, it will not be necessary for the user to make the simulation time-step smaller to

get a better result since the model is already fixed to determine the temperature stratification based on the fluid segment size. It is worthy to mention that these type of tanks are also knows as variable node tank, because a new node will be created for the inlet fluid unless the temperature difference is a certain value within the node. This type of tank is appropriate for the models based on the large degree of stratification. Type 38, is the most frequently used algebraic tank in TRNSYS (version 17 and 18).

A predetermined node tank (nodal tank) considers N isothermal nodes. The user is able to change the number of nodes. Every node has an inlet flow and outlet flow after each other, resulting in thoroughly mixing each node's current. In other word, each node isothermally interacts with nodes above and below. The differential equations, which can be driven based on each node's energy balance, are solved simultaneously at the end of each time-step in TRNSYS. These types of tanks, Type 156, 158, and 534, are the most frequent nodal tanks which are used in TRNSYS (version 18).

The type 38 for the algebraic tank and type 158 for the nodal one are investigated in this section. Our target is to investigate the outlet temperature of the both tanks and understand which one is better to produce hot water in a city with cold weather such as Toronto in Canada. We will also plot the temperature distribution and discuss about the thermocline evolution in both tanks.

3.2.1 Algebraic tank (Type 38)

This part studies the thermocline evolution along the vertical axis of the tank in both the charging and discharging mode. The tank parameters is reported in Table 3-3. Analytically speaking, the time needed for the tank to be fully charged or discharged can be calculated with the Equation 3-3 based on the fluid properties which are reported in the Table 3-4. Considering Figure 3-3 the simulation result can be compared to the analytical solution for the needed time for tank to be fully charged or discharged. It implies that after 5.4 hours, the tank reaches from its initial temperature to the entering fluid temperature for both charging and discharging mode. Consequently, Figure 3-4 qualitatively shows the thermocline evolution within the tank along the axial direction.

$$t = \frac{V\rho}{\dot{m}} = \frac{0.303 \times 1000}{56} = 5.4\ hr$$ Equation 3-3

Table 3-3 Tank Parameters for Type 38

Description	Value	Units
Tank volume ($\boldsymbol{V}$)	0.303	m^3
Tank height	1.5	m
Thermal conductivity	1.5	kj/hr/m/K
Overall Loss Coefficient	5	kj/hr/K
Initial temperature (at charging mode)	20	°C
Initial temperature (at discharging mode)	50	°C

Table 3-4 Fluid Physical Properties

Description	Value	Units
Density ($\boldsymbol{\rho}$)	1000	kg/m^3
Specific Heat	4.190	kj/kg/K
Flow-rate ($\dot{m}$)	56	kg/hr
Inlet temperature (at charging mode)	50	°C
Inlet temperature (at discharging mode)	20	°C

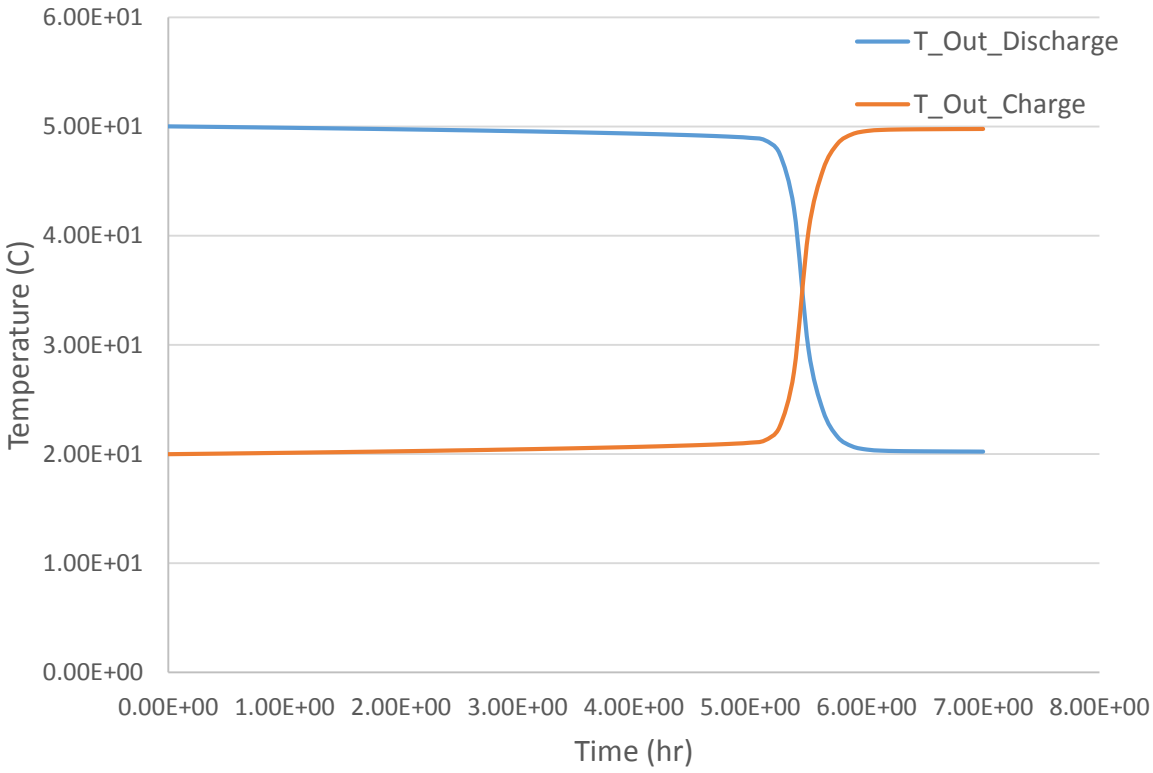

Figure 3-3 the Top Temperature of the Tank (type 38) at Charging and Discharging mode

Figure 3-4 Thermocline Evolution in Tank type 38 at a) Charging and b) Discharging mode

3.2.2 Nodal tank (Type 158)

This part investigates the thermocline evolution along the axial direction of the tank as well. The tank parameters is reported in Table 3-5 which indicates that the parameters for both of the tanks are the same. We assumed the same parameters for both types of tank in order to make a comparison on them. In light of this, the time needed for the tank to be filled is also calculated by the Equation 3-3 based on the fluid properties which are reported in the Table 3-4. Therefore, the outlet temperature behavior for this tank would be as same as the type 38. For this type tank, due to impacts of the gird spacing on the system, we are interested in investigation of temperature distribution along the height of tank at different time of simulation which are plotted in Figure 3-5 and Figure 3-7 for charging and discharging mode, respectively. Consequently, the thermocline evolution within the tank along the axial direction is shown qualitatively in Figure 3-6 and Figure 3-8 at charging and discharging mode, respectively.

Table 3-5 Tank Parameters for Type 158

Description	Value	Units
Tank volume ($\boldsymbol{V}$)	0.303	m^3
Tank height	1.5	m
Thermal conductivity	1.5	kj/hr/m/K
Top Loss Coefficient	5	kj/hr/m^2/K
Edge loss coefficient	5	kj/hr/m^2/K
Bottom loss coefficient	5	kj/hr/m^2/K
Number of Tank nodes	6	-
Initial temperature (at charging mode)	20	°C
Initial temperature (at discharging mode)	50	°C

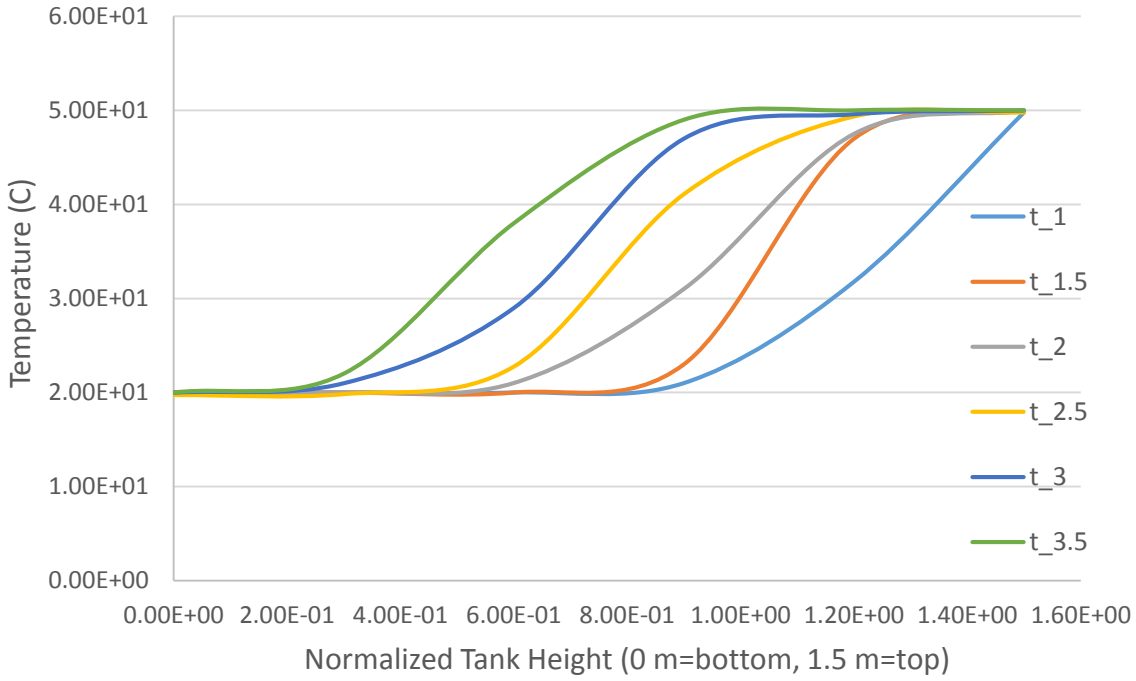

Figure 3-5 Temperature Distribution along the Height of the Tank Type 158 for a certain number of nodes at different time-step at Charging mode

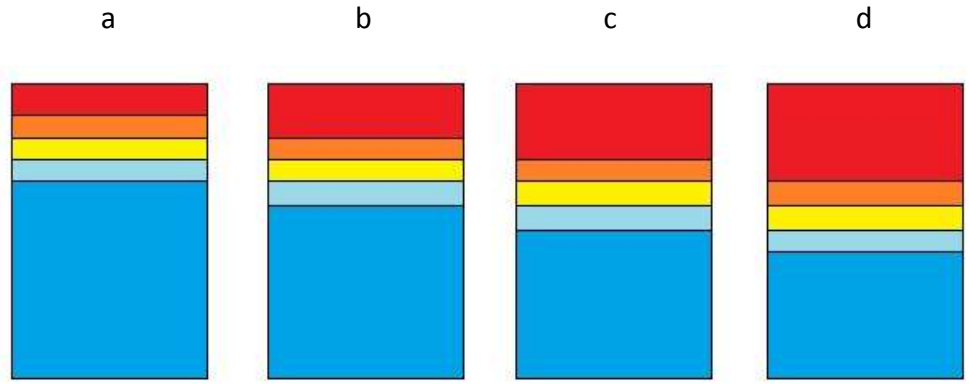

Figure 3-6 Thermocline Evolution in Tank type 158 after a) t=1 hr, b) t=1.5 hr, c) t=2 hr, and d) t=2.5 hr at Charging mode

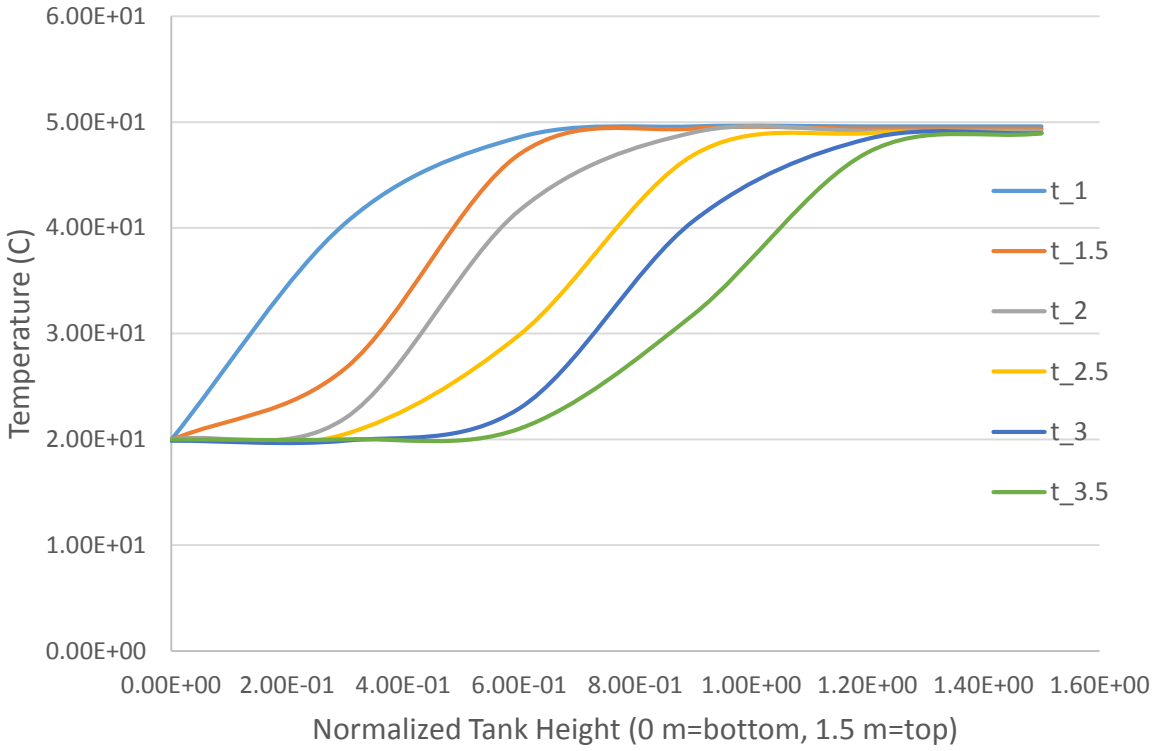

Figure 3-7 Temperature Distribution along the Height of the Tank Type 158 for a certain number of nodes at different time-step at Discharging mode

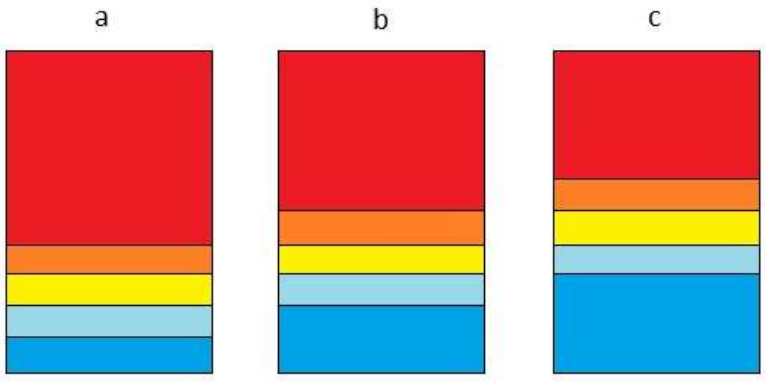

Figure 3-8 Thermocline Evolution in Tank type 158 after a) t=1.5 hr, b) t=2.5 hr, and c) t=3.5 hr at Discharging mode

3.2.3 Type 158 and Type 38 Comparison

According to the thermocline evolution figures, we concluded that tank type 158 would be better for our model to couple the solar thermal collector to the tank for providing hot water both for domestic usage and energy storing in the ground. Moreover, tank type 158 makes us able to use the auxiliary tank model in order to provide extra energy in wintertime when the useful energy gain by the solar collector is relatively low (Figure 3-2). Using the auxiliary tank model for type 158 will guarantee hot water production even in extremely cold weather places such as Toronto, ON, Canada. It is crystal clear in Figure 3-9 that using type 158 with auxiliary heat input would provide hot water at all times with a consistent temperature (approximately 60 °C) whereas the type 38 is just able to provide sufficient hot water in summertime (between Mid-April till September)(between these hours of year 2496-5832).

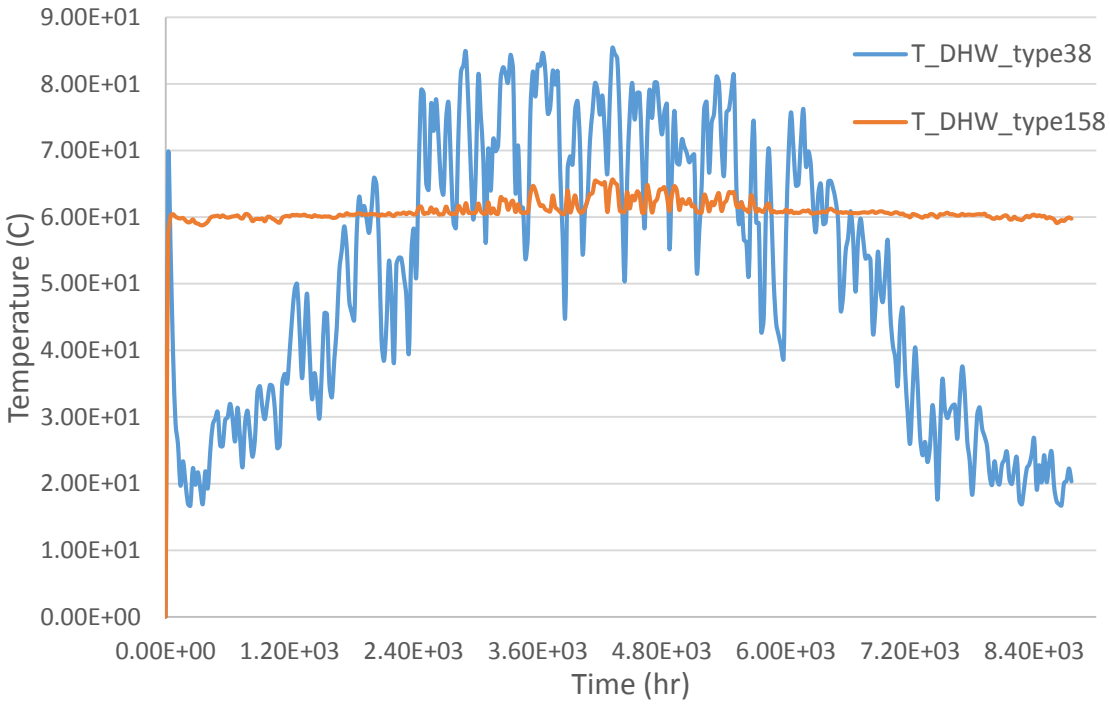

Figure 3-9 Domestic Hot Water Temperature over a year (8760 hr) for both the Tanks, Type 38 and Type 158

3.3 Borehole Heat Exchanger connected with the Heat Pump

In this subsection, a single borehole heat exchanger connected with a heat pump would provide the necessary energy for heating a single house in cold weather. Therefore, the temperature behavior of the single house and the ground soil will be investigated.

There are a few types of borehole heat exchangers in TRNSYS which are classified as vertical and horizontal. The one in which we are interested is a vertical ground heat exchanger which interacts thermally with the ground. Type 557-a is a standard U-tube ground heat exchanger through which a heat carrier fluid circulates and either rejects energy to or absorbs energy from the surrounding ground depending on the temperature differences between the fluid and the ground. In type 557-a application, after drilling a vertical borehole into the ground, an U-tube heat exchanger will be placed into the borehole. Usually, there will be a gap for several feet between the top of the ground heat exchanger and the surface of the ground. Also, there will be gap between the wall of the borehole heat exchanger and surrounding soil which will be filled by either a virgin soil or a grout depending on the geophysical properties of soils. To solve the governing equations which can be driven by the energy balance on the borehole heat exchanger influenced by different forms of heat transfer, including convection within the pipes, conduction to the storage volume, TRNSYS assumes that the U-tube borehole heat exchanger is pushed uniformly within the ground storage volume. TRNSYS calculates the ground (soil) temperature by using a superposition method between three parts. The global and local temperature which can be calculated using an explicit FDM, and the steady flux solution which can be found analytically [27]. Type 557-a parameters and characteristics used in the model is reported in Table 3-6.

TRNSYS provides a few types of heat pumps too, which are classified as water-source and water-water heat pumps. The heat transfer would take place between the moist air and liquid stream in the former, and it transfers between two different liquid streams in the latter. Type 1221 is a two-stage water-water heat pump which rejects heat in heating mode and absorbs heat in cooling mode from one liquid stream to another. In this heat pump, TRNSYS provides the cooling control and heating control signals, allowing the system to operate at different temperature levels. This makes the user able to define and set different temperature dead bands, based on the season of the year, to switch the heat pump from cooling mode (in

summer) to heating mode (in winter), or vice versa. Therefore, the system or the model would operate at its capacity, whether it is on the cooling mode or on the heating mode, until the control signal value changes [27]. The temperature set pointes has been defined in a way that we get 18 to 22 °C in the winter time and 23 to 27 °C in summer time for a house temperature in Toronto, ON, Canada. These temperature set points of the heat pump type 1221 are reported in Table 3-7 based on the controller type 108 values. This controller is a five stage thermostat which sends 0 as off and 1 as on signals to heat pump based on these temperature set points that can be defined by the user. The source liquid stream is considered as ethylene glycol solution 60 % and the load liquid stream is considered as water whose physical properties are also reported in Table 3-7.

Table 3-6 Borehole Heat Exchanger Type 557-a Parameters and Characteristics with the Heat Carrier Fluid

Description	Value	Units
Storage Volume	6000	m^3
Borehole Depth	150	m
Header Depth	1	m
Number of Boreholes	1	-
Borehole Radius	0.1016	m
Number of Boreholes in Series	1	-
Storage Thermal Conductivity	4.68	kj/hr/m/K
Storage Heat Capacity	2016.0	$kj/m^3/K$
Outer Radius of U-Tube Pipe	0.01664	m
Inner Radius of U-Tube Pipe	0.01372	m
Center-to-Center Half Distance	0.0254	m
Fill Thermal Conductivity (grout)	4.68	kj/hr/m/K
Pipe Thermal Conductivity	1.5122	kj/hr/m/K

Fluid Specific Heat	3.284	kj/kg/K
Fluid Density	1095	kg/m^3
Flow rate of Fluid	30	kg/hr
Initial Surface Temperature of Storage Volume	14	°C

Table 3-7 Liquid Streams Physical Properties and Temperature Set Points of the Thermostat type 108 for Switching the Type 1221 from Cooling to Heating mode, and vice versa

Description	Value	Units
Source Fluid Specific Heat	3.284	kj/kg/K
Source Fluid Density	1095	kg/m^3
Source Flow rate	30	kg/hr
Load Fluid Specific Heat	4.190	kj/kg/K
Load Fluid Density	1000	kg/m^3
Load Flow rate	30	kg/hr
Heating set point Temperature	20	°C
Cooling set point Temperature	25	°C
Temperature dead band	4	delta °C

3.3.1 Single House (Type 12-c)

Among the different components for loads and structure in TRNSYS, Type 12c models a single house which is used in our model. The corresponding parameters for a single house in this component are reported in Table 3-8. In order to analytically investigate the temperature profile of the house, we can write the energy balance on the house based on Figure 3-10. Driving the energy balance on the house (Equation 3-4), we will understand that at different conditions of heat pump, whether it is on or off, the house temperature would behave either exponentially or linearly. As described in Equation 3-5, when the heat pump is off, we would have just the heating loss term in our energy balance equation, resulting in exponential behavior of the house temperature with respect to time. However, considering Equation 3-6, when the heat pump is on, both heating loss and energy from/to heat pump terms would be in the energy balance, resulting in a linear relation between the house temperature and time.

Table 3-8 Single House (type 12-c) Characteristics and Parameters

Description	Value	Units
Overall loss coefficient of house	600	kj/hr/K
House thermal capacitance	18000	kj/K
Initial room temperature	20	°C
Specific heat of source fluid	4.190	kj/kg/K
Effectiveness-Cmin product	200	kj/hr/K
Latent heat ratio	0.23	-

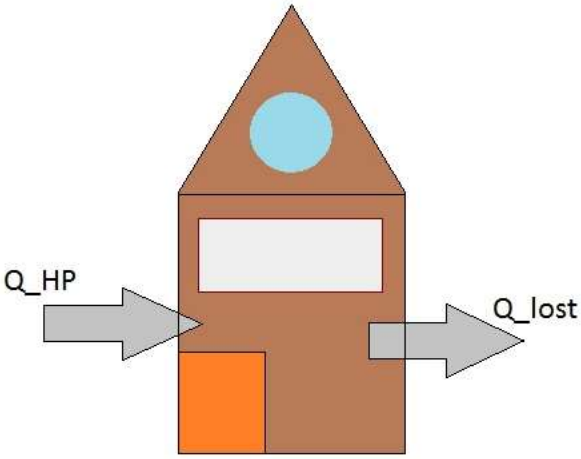

Figure 3-10 Schematic of a Single House (type 12c) and its Thermal Interact with Surrounding

$$mC_p \frac{dT_{house}}{dt} = Q_{HP} - Q_{lost} = Q_{HP} - UA(T_{h,i} - T_\infty) \quad \text{Equation 3-4}$$

$$\Rightarrow \quad \frac{dT_{house}}{dt} = \frac{Q_{HP}}{mC_p} - \frac{UA}{mC_p}(T_{h,i} - T_\infty)$$

If $T_{house} > T_{hot\_controller}$, then the heat pump is OFF, so: $Q_{HP} = 0$. Equation 3-4 is rewritten as follows:

$$\frac{dT_{house}}{dt} = -\frac{UA}{mC_p}(T_{h,i} - T_\infty) \quad \Rightarrow \quad T_{house}(t) \simeq \exp(t) \quad \text{Equation 3-5}$$

If $T_{house} < T_{hot\_controller}$, then the heat pump is ON, so: $Q_{HP} \neq 0$. Solving Equation 3-4 would result in a linear relationship between temperature and time as follows:

$$T_{house}(t) = \frac{Q_{HP}}{mC_p}\, t + Constant \quad \text{Equation 3-6}$$

3.3.2 Simulated Model Results

We modeled the system for a day in winter (January 1st) and we compared the room temperature results with the analytical results which is plotted in Figure 3-11. It can be implied that simulation results are pretty aligned with the analytical ones. In the plot, when the heat pump is off, the temperature of the room would decrease exponentially until it reaches the minimum set point temperature value of the thermostat (type 108), which is 18 °C. However, while the heat pump is on, the room temperature would increase linearly until

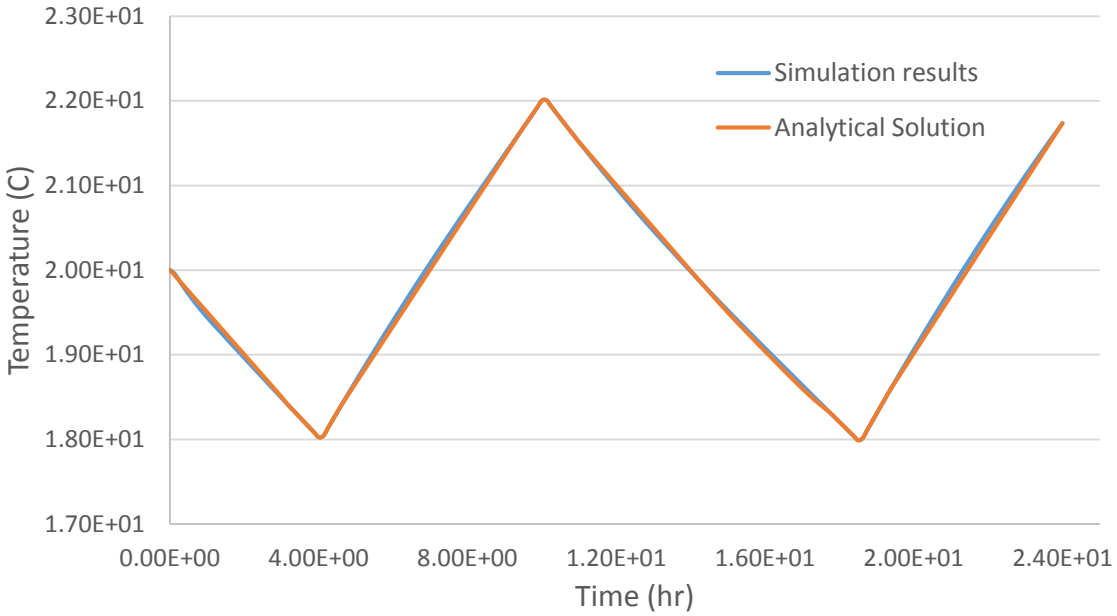

Figure 3-11 Simulation and Analytical Results of the Room Temperature for a Single House (type 12-c) in TRNSYS

it reaches the maximum set point temperature value of the thermostat, which is 22 °C in winter-time.

Last but not least, a model for the borehole heat exchanger (type 557a) connected to the heat pump (type 1221) for a single house (type 12-c) for Toronto city in Canada is simulated in TRNSYS. In this model, we investigated the effect of borehole depth on the average soil temperature by using three different values (100, 150, and 200 m) for borehole depth, an then we plotted our results in Figure 3-12. Lastly, we qualitatively compared our results with Tian et al [13], Figure 3-13 is coming from this work. By comparing Figure 3-12 and Figure 3-13, we can imply that over ten years of using the ground as the heat source, the soil temperature would decrease regardless of the borehole depth. However, it is crystal clear that the more the borehole depth, the less the soil temperature decline.

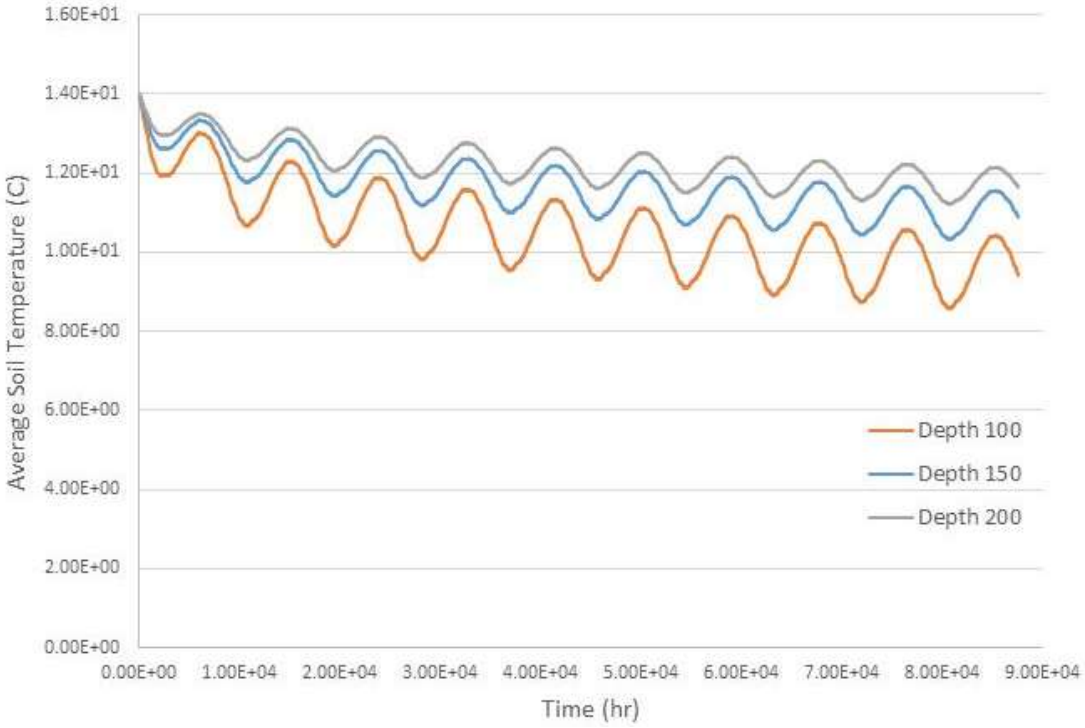

Figure 3-12 Average Soil Temperature over Ten years for Different Borehole Depth, current study

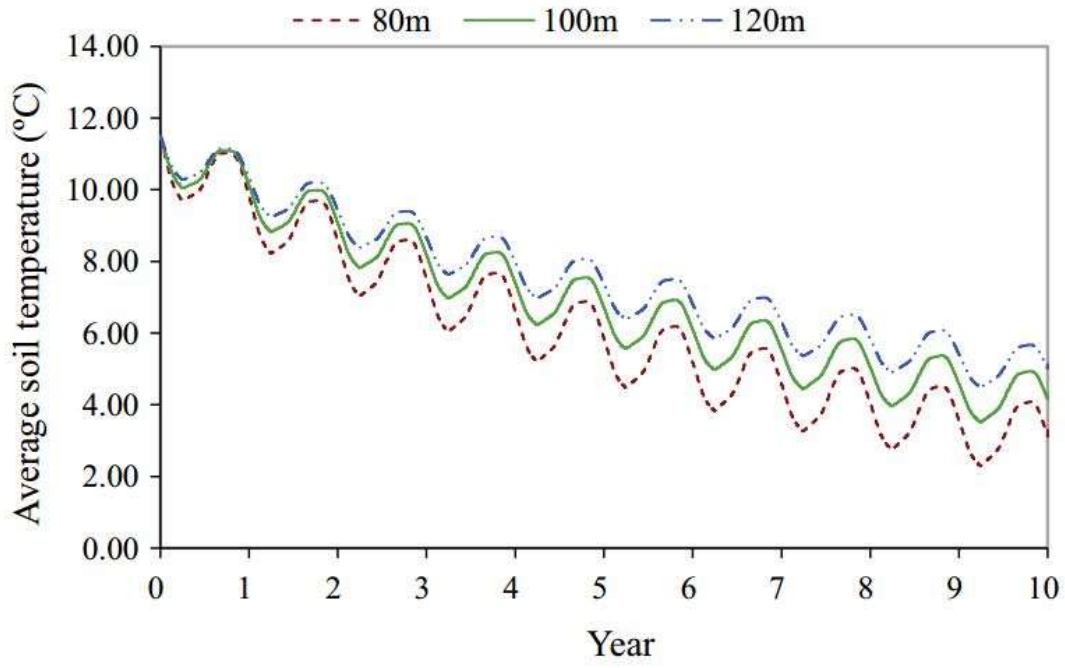

Figure 3-13 Average Soil Temperature over Ten years for Different Borehole Depth, Tian et al study [13]

3.4 Conclusion

This chapter was dedicated to identifying the most important components which are used in our work. Their parameters, characteristics, types, and descriptions have been discussed. Based on the literature and typical applications, we came up with these components and conducted some models separately for each subsection of this chapter. The results showed that these components are the ones we should choose for our study, and the models we investigated are running correctly. In the next chapter, we will show the final results of our work, and we will see how these models fulfill our target if we couple them with each other.

Chapter 4
Results and Discussion

As we identified before in Chapter 3, we chose to use type 1b as the solar thermal collector, type 158 as the storage tank, type 557a as the borehole heat exchanger, type 1221 as the heat pump, and type 12-c as the single house in our model. The corresponding parameters have been reported in Table 3-1, Table 3-5, Table 3-6, Table 3-7, and Table 3-8, respectively. The simulation is conducted over ten years.

In this chapter, we will measure different values and outcomes of our project-work, such as the Solar Domestic Hot Water (SDHW) system performance—which is described as solar fraction—, solar thermal collector efficiency, inlet and outlet temperatures of flowing streams within the storage tank, DHW temperature profile, the total heat transfer rate between the fluids in the counter-flow heat exchanger, room temperature profile of the single house, and the soil temperature fluctuation. Then, we will discuss the results to see whether our goal in this project, which is improving the ground thermal imbalances, is satisfied or not. For all of these purpose, we used TRNSYS which is a commercial tool for simulating and solving the transient system [27]. A simple schematic of our model is shown in Figure 4-1.

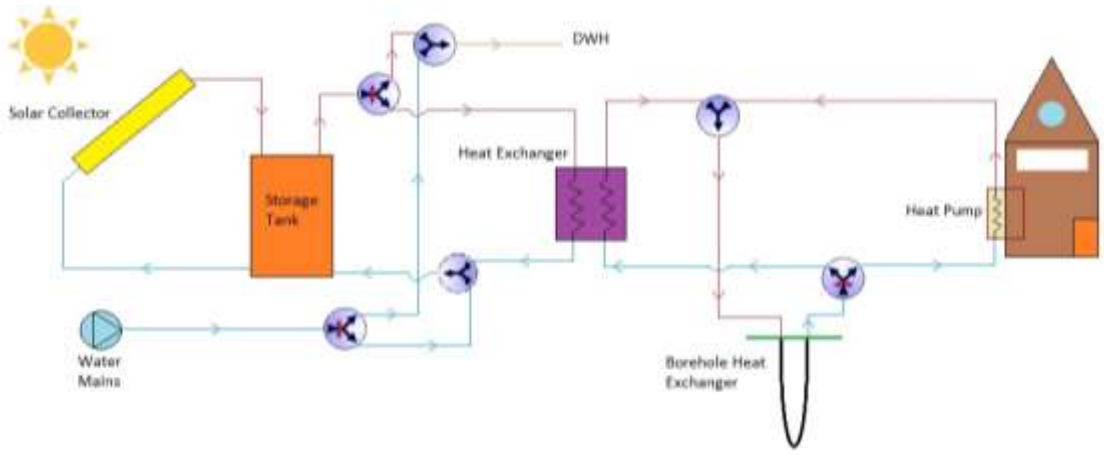

Figure 4-1 Model Schematic of the Current Study, Solar Thermal Collector Coupled with the Ground Source Heat Pump

4.1 Solar Fraction

Solar fraction is a parameter which shows the performance of the solar collector. Solar fraction can be calculated by diving the energy coming from the sun by the load energy, Equation 4-2. The load energy is the necessary energy for proving the hot water. In our model, because we are considering the model for a cold weather city, Toronto, we used an auxiliary model for the storage tank to compensate the lack of energy coming from the sun in wintertime. Therefore, the load energy would be equal to summation of both the energy coming from the sun and the auxiliary energy. Equation 4-1 is written based on this definition. It is noteworthy that the load energy is symbolized as $Q_{load} = Q_{DHW}$.

$$Q_{DHW} = Q_{sun} + Q_{aux} \Rightarrow Q_{sun} = Q_{DHW} - Q_{aux} \quad \text{Equation 4-1}$$

$$F_S = \frac{Q_{sun}}{Q_{DHW}} = 1 - \frac{Q_{aux}}{Q_{DHW}} \quad \text{Equation 4-2}$$

After 4920 hours of simulation, which would be around end of July, the solar fraction has been computed according to the Equation 4-2 and it is equal to 0.58 (58 %). Based on the literatures and real applications, solar fraction values should be around 60 % for a good performance in a solar thermal system in Toronto, ON, Canada [16].

4.2 Solar Thermal Collector Efficiency

This parameter indicates whether the solar collector is performing at its best condition. This numerical factor highly depends on the inlet and outlet temperature of the circulating fluid, which is solution of ethylene glycol and water whose physical parameters are reported in Table 3-2. The more the outlet temperature, the higher the efficiency. Also, the less the inlet temperature, the higher the efficiency. This implies that, if the fluid enters the solar collector with lower temperature, the solar collector could transfer more energy to the fluid which is gained from the sun, so the higher the rate of this heat transfer, the higher the efficiency of

the solar collector. In other words, as the heat transfer increases between the circulating fluid and the solar collector within the solar collector, the useful energy gained by the collector increases too. Accordingly, the efficiency, which is a fraction between the useful energy gain and the total radiation incident on the solar collector, would increase, based on the Equation 3-2.

After a 4920-hour simulation, which would be around end of July, the solar thermal collector efficiency has been computed based on the Equation 4-3 and it is equal to 0.66 (66 %).

$$\eta = \frac{Q_u}{A_C G_T}$$ Equation 4-3

4.3 Storage Tank Streams' Temperatures Profile

There are two different liquid streams within the storage tank; one is coming from the solar thermal collector, which contains the essential energy for rejecting to the second stream for proving hot water, and the second stream is water supplied by the mains. There are two inlet and two outlet ports on the storage tank. Each stream enters the tank from one of the inlet ports and exits from one of the outlet ports. Therefore, there would be four different temperatures which are attractive to take a look at their values. Figure 4-2 and Figure 4-3 shows these temperatures' behavior for one year as the simulation start and stop time. Although the inlet temperature of the fluid coming from the solar collector is below 0 °C in wintertime and above 100 °C in summertime, the fluid would not freeze in winter or boil in summer as the freezing and boiling point of the ethylene glycol solution are -52.8 °C and 111.1 °C, respectively.

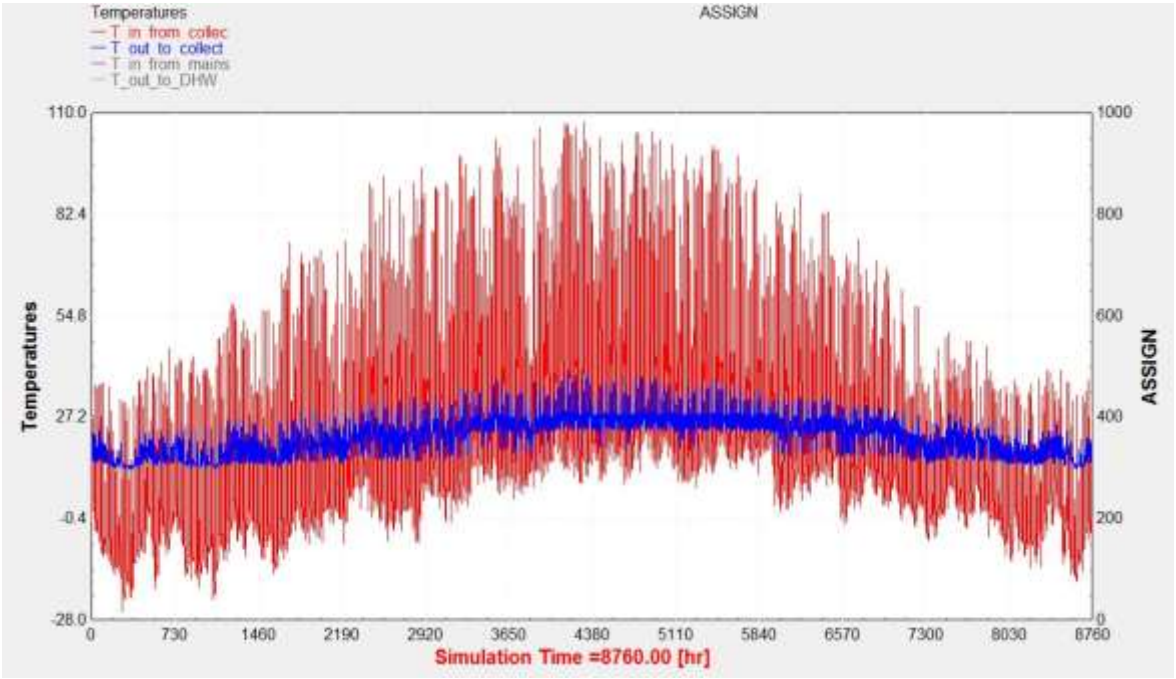

Figure 4-2 Inlet and Outlet Temperature of the Circulating Fluid through the Storage Tank and Solar Collect

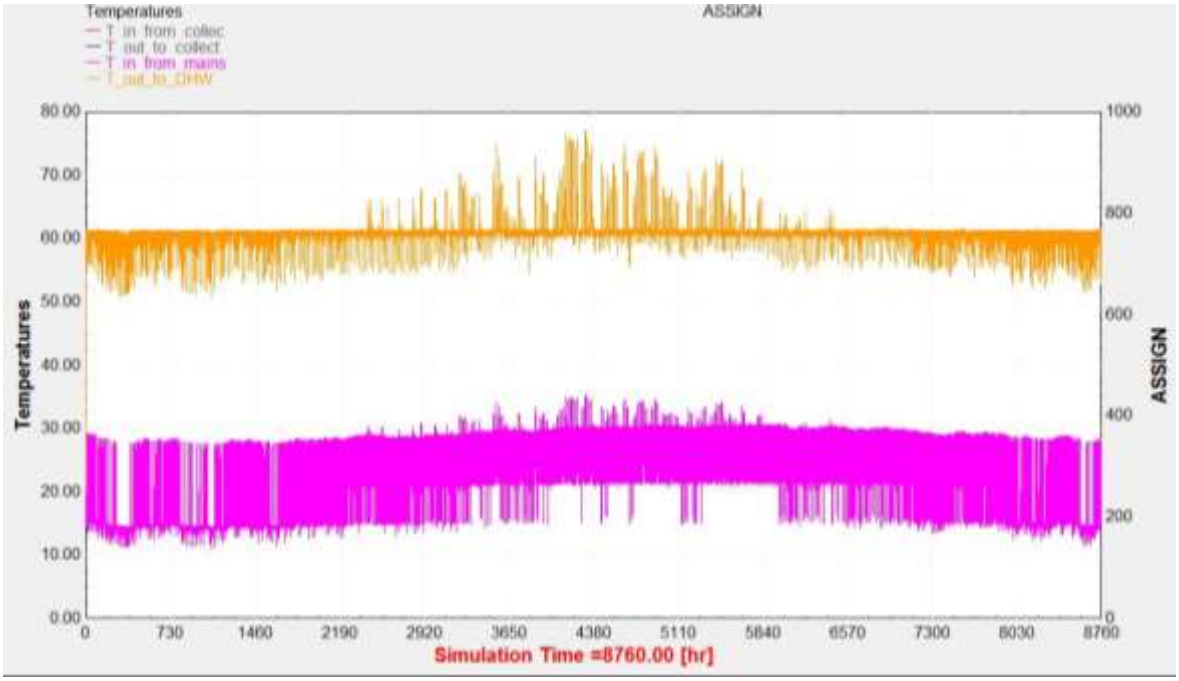

Figure 4-3 DHW Temperature as the Outlet of the Storage Tank and Temperature Fluctuation of the Mixture of Water, Coming from the Mains and the Heat Exchanger

4.4 Domestic Hot Water Temperature Profile

In daily usage of a house, hot water is used to be mixed with cold water to increase the temperature of the water aimed at domestic needs such as washing and cleaning. For this purpose, we use a mixer in our model which adds cold water supplied by the water mains to the outlet stream coming from storage tank. Figure 4-4 shows the temperature differences between the hot water before and after mixing with cold water. It can be implied that the average hot water temperature over a year is around 61 °C before mixing and 56 °C after mixing. It is worthy of mentioning that, to reducing the DHW temperature even lower than 56 °C, we can easily increase the cold water flow rate.

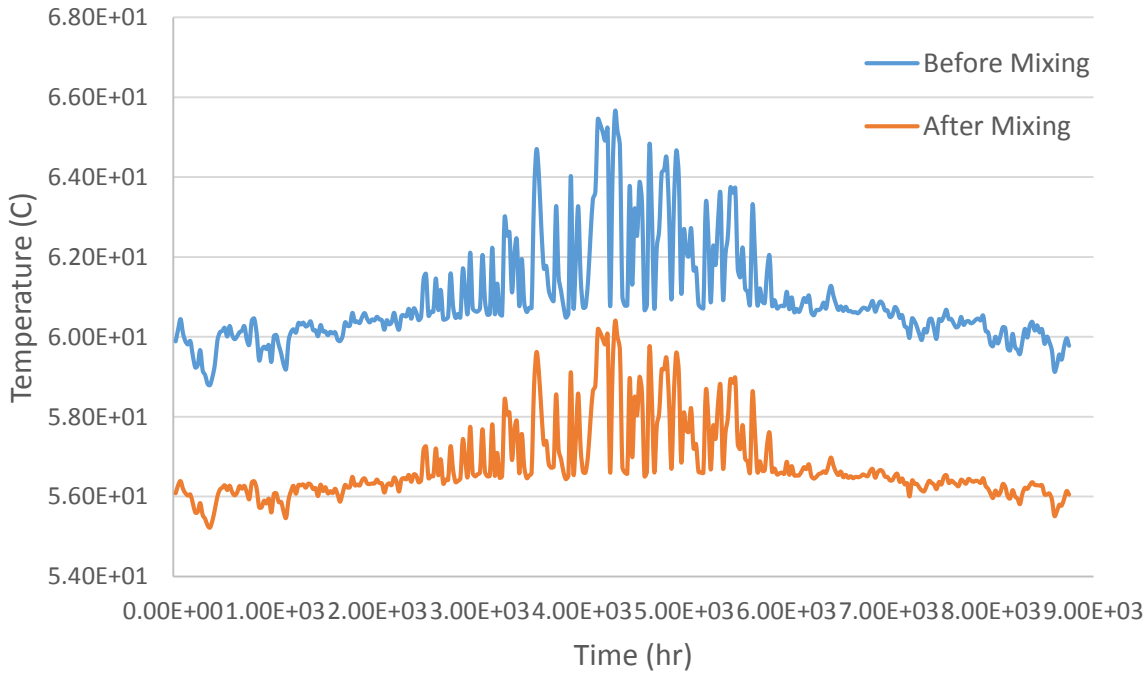

Figure 4-4 Hot Water Temperature Behavior before and after getting mixed with Cold Water Supplied by Water Mains

4.5 Heat Exchanger Performance

In order to coupling the solar thermal system with ground source heat pump, we decided to use a heat exchanger in our model. TRNSYS provides a number of heat exchangers which are modeled in various configurations [27]. Type 5b, whose parameters is reported in Table 4-1, is a counter flow heat exchanger in which its effectiveness will be calculated based on a certain value of the overall heat transfer coefficient, a design parameter assigned by the user (UA), with respect to the inlet temperatures and flow rates of the hot and cold side. Equation 4-4 shows how TRNSYS calculates the effectiveness of a counter flow heat exchanger. A simple schematic of this type of heat exchanger is shown in Figure 4-5.

$$\varepsilon = \frac{1-\exp\left[-\frac{UA}{C_{min}}\left(1-\frac{C_{min}}{C_{max}}\right)\right]}{1-\left(\frac{C_{min}}{C_{max}}\right)\exp\left[-\frac{UA}{C_{min}}\left(1-\frac{C_{min}}{C_{max}}\right)\right]} \qquad \text{Equation 4-4}$$

Where, $C_{min} = \min(C_c, C_h)$ and $C_{max} = \max(C_c, C_h)$, in which $C_c = \dot{m}_c C_{p_c}$ and $C_h = \dot{m}_h C_{p_h}$ are defined as cold side and hot side capacitance of the heat exchanger, respectively.

Table 4-1 Counter Flow Heat Exchanger (type 5b) Parameters

Description	Value	Units
Specific heat of source side fluid	4.190	kj/kg/K
Specific heat of load side fluid	3.284	kj/kg/K
Overall heat transfer coefficient of exchanger	1000	kj/hr/K
Mass flow rate of source side fluid	30	kg/hr
Mass flow rate of load side fluid	30	kg/hr

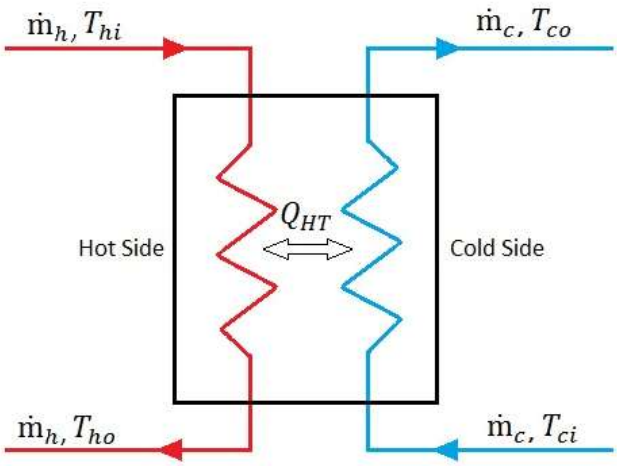

Figure 4-5 Schematic of a Counter Flow Heat Exchanger and its Circuits

The simulation results for each stream's inlet and outlet temperature, and the heat transfer rate of the heat exchanger (type 5b) are plotted in Figure 4-6, Figure 4-7, and Figure 4-8, respectively. Considering these figures, it can be implied that the heat exchanger performance is quite acceptable since the hot stream enters the heat exchanger with a high temperature (whose average temperature over a year is 61 °C) and leaves it with a lower one (the average of which is equal to 24.5 °C over a year). This happens for the cold fluid on the load side of the heat exchanger as well (the average temperatures of cold fluid for inlet and outlet are 14.5 and 60 °C over a year, respectively). Additionally, the outlet temperature of the hot fluid fluctuation in the summertime differs from that of in the wintertime; this is simply because, in the summertime, the storage tank would provide DHW with higher temperature such that a portion of which directly enters the hot side of the heat exchanger on the one hand, and on the other hand, the inlet temperature of the cold fluid increases too due to the heat rejection in the borehole heat exchanger which takes place in the summertime, resulting in lower heat transfer rate in the heat exchanger. Simulation results demonstrated that the minimum heat transfer rate for the first year of simulation is 3805.4 kj/hr (in summer, September), and its maximum value is 5729.6 kj/hr (in winter, February). Also, the average value of the heat transfer rate over a year is about 4564.3 kj/hr. Finally, it is worth noting that the simulation results for effectiveness have a reasonable value for this kind of heat transfer we used in our model, the value of which is around 0.9736.

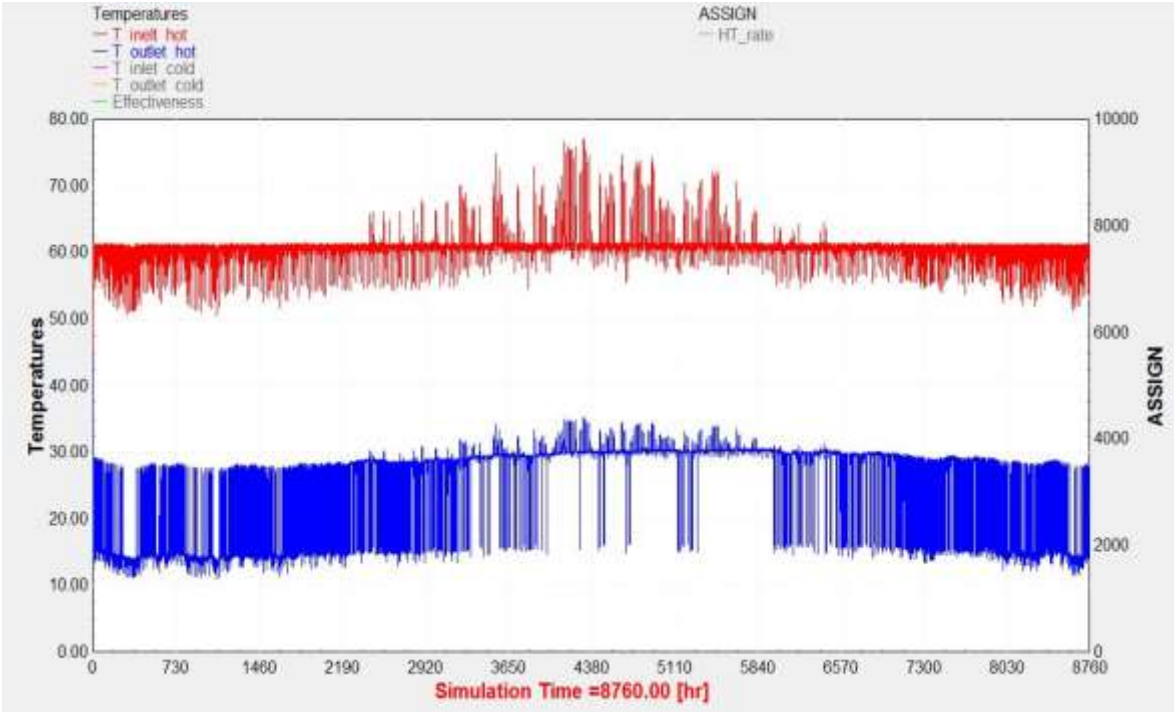

Figure 4-6 the Inlet and Outlet Temperature of the Counter Flow Heat Exchanger (type 5b) in the Source Side (Hot Side)

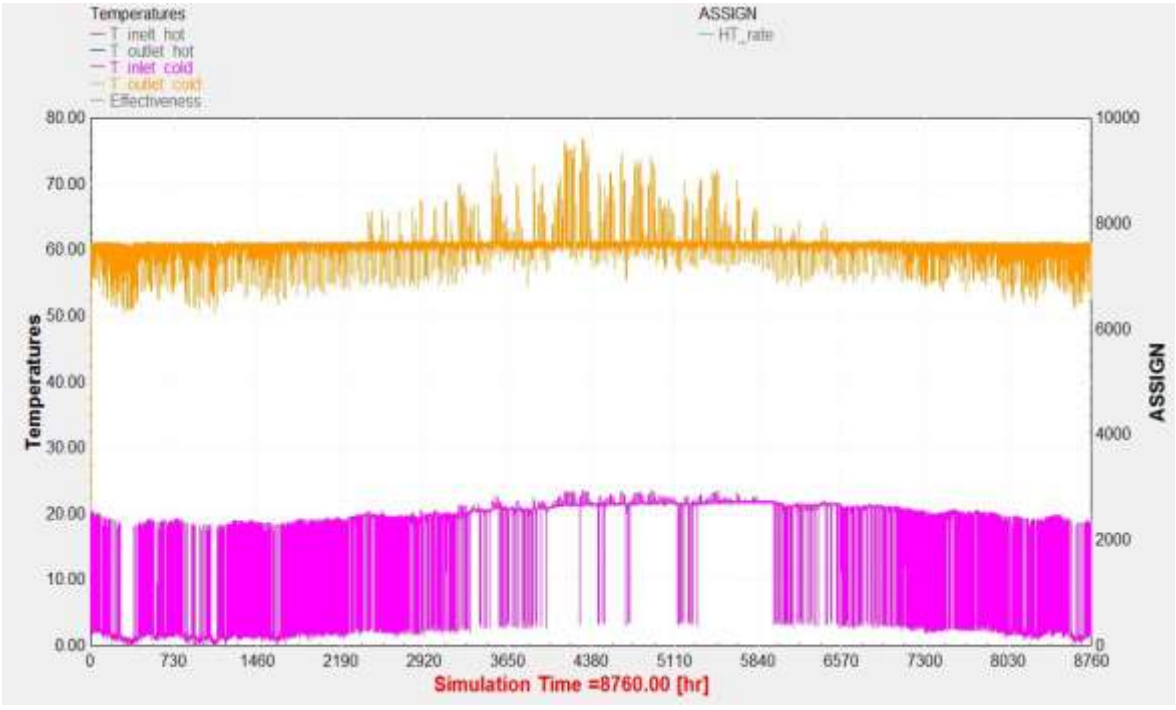

Figure 4-7 the Inlet and Outlet Temperature of the Counter Flow Heat Exchanger (type 5b) in the Load Side (Cold Side)

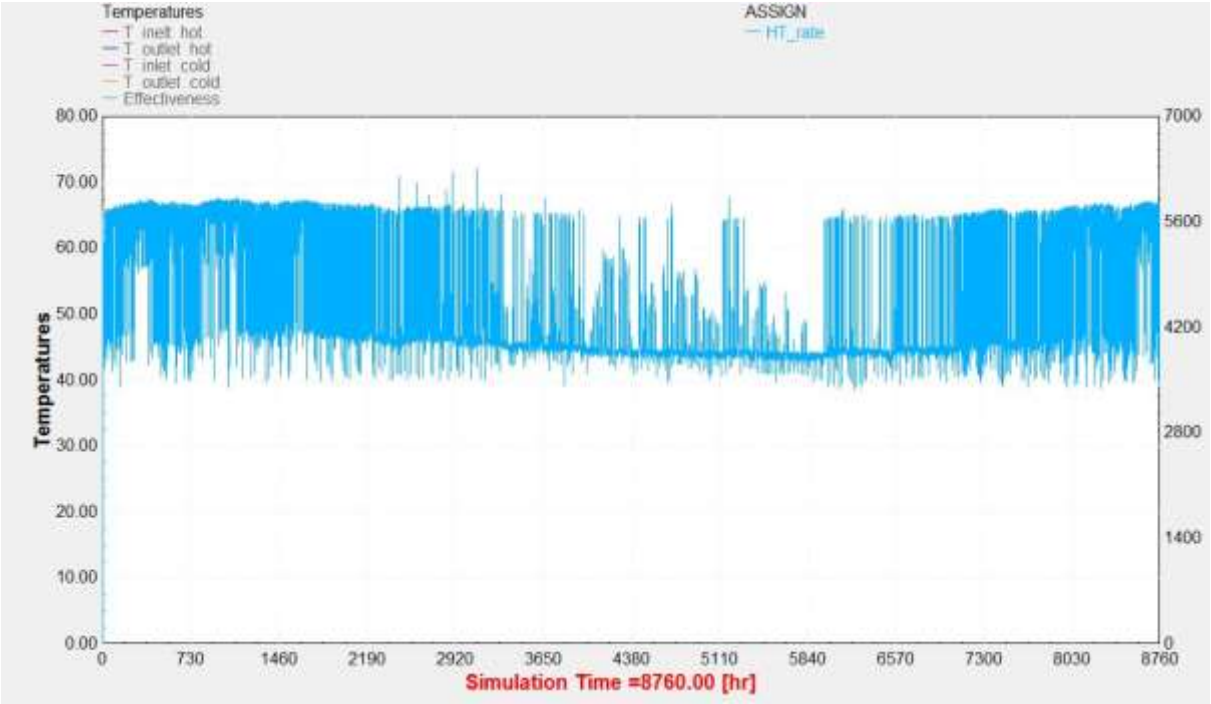

Figure 4-8 the Heat Transfer Rate of the Counter Flow Heat Exchanger (type 5b)

4.6 Room Temperature

As already described in subsection 3.3.1 and Equation 3-4 the room temperature would fluctuate either linearly or exponentially with respect to the time. We should be aware that the room temperature profile would have the same behavior for each simulation year. Thus, we just presented the simulation result for this parameter for the first year of simulation in Figure 4-9. It should be noted that the room temperature is changing between the set point values of the thermostat, which are assigned according to the comfort temperature range. The comfort temperature for a house is considered to be between 18 °C to 22 °C in winter and 23 °C to 27 °C in summer for a heating-dominant city like Toronto, ON, Canada. Figure 4-9 also shows the results for the heating control signal. It can be implied that whenever the heat pump is on heating mode, the heating control signal is 1, the room temperature is in the range of 18 °C and 22 °C representing the wintertime, and vice versa.

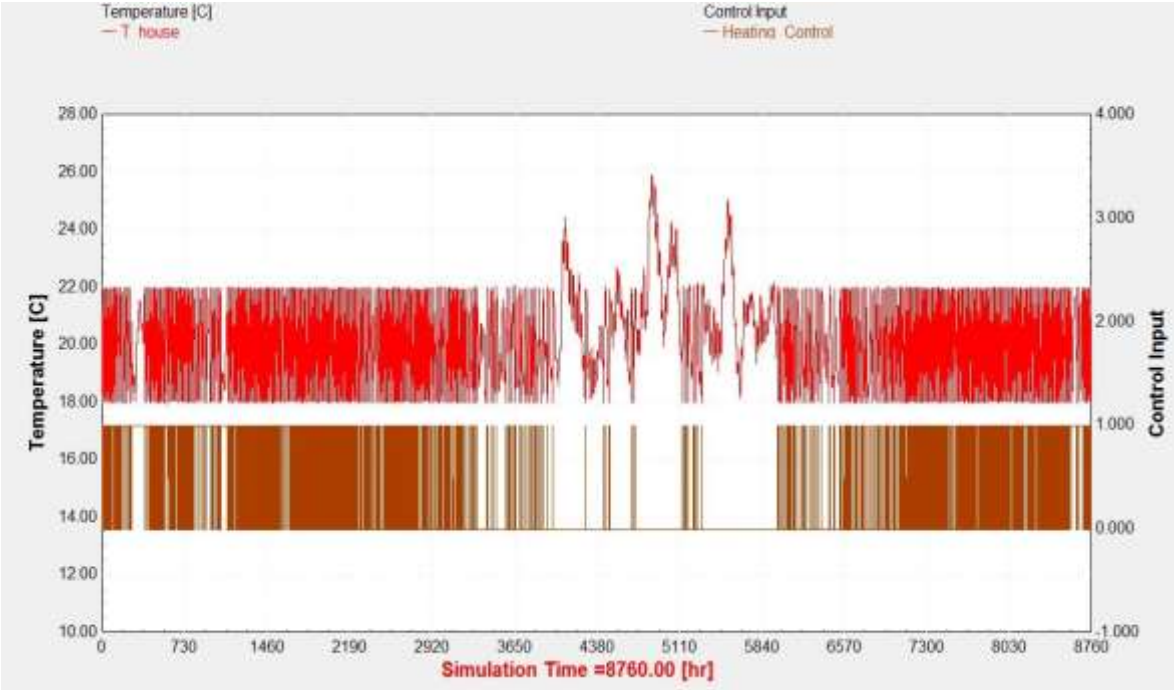

Figure 4-9 Simulation results for Room Temperature Profile and Heating Control Signal with respect to the Time

4.7 Soil Temperature

The critical parameter of our interest in this study is the soil temperature fluctuations over ten years of simulation time. Using the ground as a heat source for space heating would decrease the soil temperature by the passage of time, such that the ground would not be able to reject heat for this purpose. As discussed before in subsection 3.3.2, for a Ground Source Heat Pump (GSHP) system, whose parameters are reported in Table 3-6, the soil temperature reduces by 22.2 % from its initial after ten years of operation (this result can also be implied from Figure 3-12). By coupling the solar domestic hot water to the ground source heat pump, we conclude that the soil temperature reduction is just for 3.6 % of its initial value over a ten-year operation. The differences between the final values of the soil temperature for a GSHP and a Solar Domestic Hot Water System Coupled with Ground Source Heat Pump (SDHWSCGSHP) over ten years are plotted in Figure 4-10. The soil temperature increases from 10.88 °C to 13.49 °C which is equivalent to 24 % of increment.

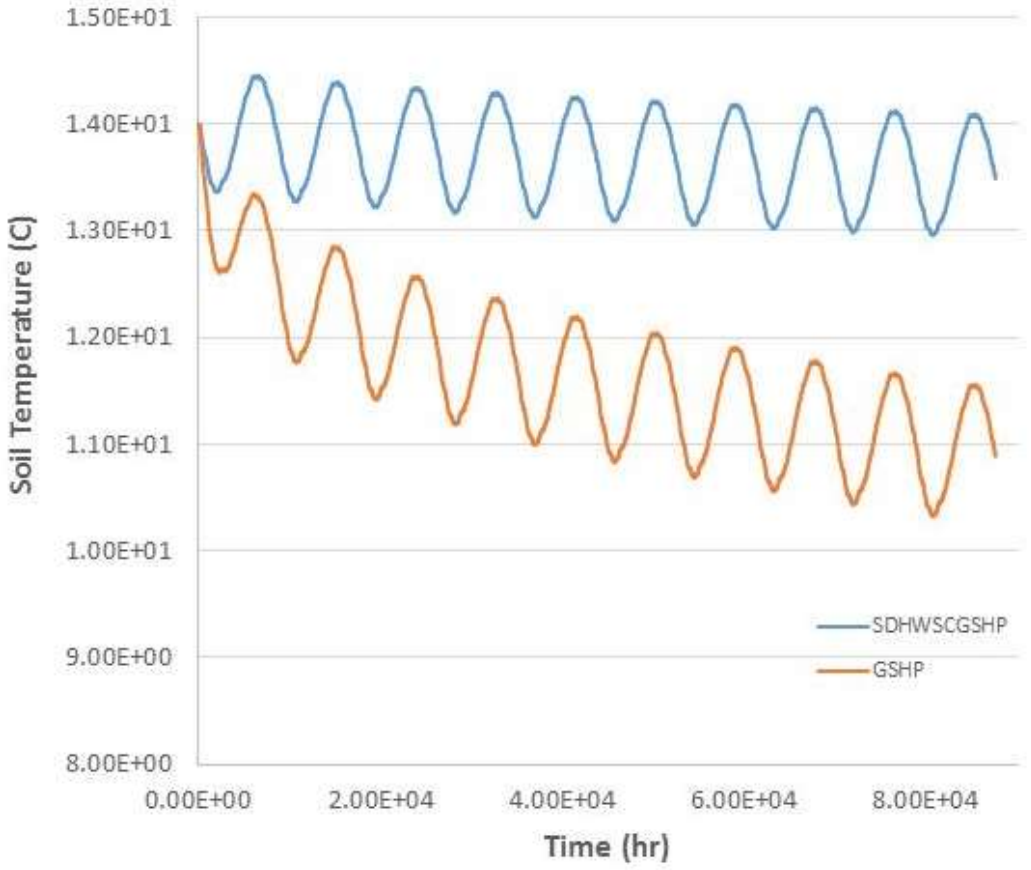

Figure 4-10 Soil Temperature Fluctuation for two Different Systems, Simulated in TRNSYS for Ten Years in Toronto, ON, Canada

4.8 Conclusion

Using ground source heat pumps for space heating in heating-dominated climates, such as Canada, would result in soil thermal capacity decline, and this is simply because more energy is extracted from the ground in the winter than is stored in the summer. This study aimed to investigate one of the possible ways to improve the soil temperature by using a green source of energy, which is the sun. Solar thermal collectors are widely used in the production of domestic hot water in Canada. Thus, the coupling of an existing solar domestic hot water system with an existing ground source heat pump in this study proved that this idea could be a reliable solution to mitigate the soil thermal capacity by the passage of time. Results

demonstrated that using this system would increase the soil's temperature by 24 % after a ten-year operation. Therefore, after a long-term operation period, there will be no need for a solar domestic hot water system coupled with a ground source heat pump (SDHWSCGSHP) system to drill another borehole heat exchanger into the ground due to the system performance decline, which is a result of soil thermal decline itself. Drilling a borehole into the ground is a costly operation, especially in cold weather countries where the borehole should be pushed deeply into the ground to reach higher values of soil temperature. Consequently, the SDHWSCGSHP system is also economically advantageous.

This study has been conducted for a single house in Canada with a U-tube borehole heat exchanger whose length is 150 m. This work could also be done on Multi-Family House (MFH). The effect of borehole length on the soil temperature in different locations over different operation time could also be investigated in future works.

Nomenclature and Acronyms

Nomenclature

Symbols	Definitions	Units
Q_u	Rate of Useful Energy Gain	kj/hr
A_C	Collector Area	m^2
$F_R(\tau\alpha)$	Intercept Efficiency	-
G_T	Total radiation incident on the solar collector (Tilted surface)	$kj/hr/m^2$
$F_R U_L$	Efficiency Slope	$kj/hr/m^2/K$
T_i	Collector inlet temperature	°C
T_a	Ambient temperature	°C
η	Solar thermal collector efficiency	-
T_o	Outlet Temperature	°C
t	Time	hr
V	Volume	m^3

ρ	Density	kg/m^3
$\dot{m}$	Flow rate	kg/hr
C_p	Specific Heat	kj/kg/K
Q_{HP}	Energy absorbed from or rejected to Heat Pump	kj/hr
Q_{lost}	Energy loss from the system	kj/hr
UA	Overall Heat Transfer Coefficient	kj/hr/K
U	Heat Loss Coefficient	kj/hr/m^2/K
$T_{h,i}$	Initial Temperature of House	°C
T_∞	Ambient Temperature	°C
Q_{DHW}	Necessary Energy for Producing Domestic Hot Water	kj/hr
Q_{sun}	Energy Coming from the Sun	kj/hr
Q_{aux}	Auxiliary Energy Input	kj/hr
F_s	Solar Fraction	-
C	Heat Exchanger Capacitance	kj/hr/K
C_{min}	Minimum Capacitance	kj/hr/K

C_{max}	Maximum Capacitance	kj/hr/K
ε	Heat Exchanger effectiveness	-

Acronyms

Symbols	**Definitions**
TRNSYS	Transient System Simulation
SDHW	Solar Domestic Hot Water
GSHP	Ground Source Heat Pump
CSCGHP	Combined Solar Collector-Geothermal Heat Pump
FDM	Finite Difference Method
DLSC	Drake Landing Solar Community
SAGSHPGHS	Solar Assisted Ground-Source Heat Pump Greenhouse Heating System
SAGSHP	Solar Assisted Ground-Source Heat Pump
LHEST	latent heat energy storage tank
COP	Coefficient of Performance
MFH	Multi-Family Houses

SDHWSCGSHP	Solar Domestic Hot Water System Coupled with Ground Source Heat Pump

Bibliography

1. Kjellsson, E., Hellström, G., & Perers, B. (2010). Optimization of systems with the combination of ground-source heat pump and solar collectors in dwellings. Energy, 35(6), 2667-2673.
2. Chargui, R., & Sammouda, H. (2014). Modeling of a residential house coupled with a dual source heat pump using TRNSYS software. Energy Conversion and Management, 81, 384-399.
3. Mehrpooya, M., Hemmatabady, H., & Ahmadi, M. H. (2015). Optimization of performance of Combined Solar Collector-Geothermal Heat Pump Systems to supply thermal load needed for heating greenhouses. Energy Conversion and Management, 97, 382-392.
4. Emmi, G., Zarrella, A., De Carli, M., & Galgaro, A. (2015). An analysis of solar assisted ground source heat pumps in cold climates. Energy Conversion and Management, 106, 660-675.
5. Chen, X., & Yang, H. (2012). Performance analysis of a proposed solar assisted ground coupled heat pump system. Applied energy, 97, 888-896.
6. Ozgener, O., & Hepbasli, A. (2005). Experimental performance analysis of a solar assisted ground-source heat pump greenhouse heating system. Energy and Buildings, 37(1), 101-110.
7. Rad, F. M., Fung, A. S., & Leong, W. H. (2013). Feasibility of combined solar thermal and ground source heat pump systems in cold climate, Canada. Energy and Buildings, 61, 224-232.
8. Safa, A. A., Fung, A. S., & Kumar, R. (2015). Heating and cooling performance characterization of ground source heat pump system by testing and TRNSYS simulation. Renewable Energy, 83, 565-575.
9. Han, Z., Zheng, M., Kong, F., Wang, F., Li, Z., & Bai, T. (2008). Numerical simulation of solar assisted ground-source heat pump heating system with latent heat energy storage in severely cold area. Applied Thermal Engineering, 28(11-12), 1427-1436.
10. Eslami-Nejad, P., & Bernier, M. (2011). Coupling of geothermal heat pumps with thermal solar collectors using double U-tube boreholes with two independent circuits. Applied Thermal Engineering, 31(14-15), 3066-3077.
11. Metz, P. D. (1982). The use of ground-coupled tanks in solar-assisted heat-pump systems.
12. Emmi, G., Zarrella, A., De Carli, M., & Galgaro, A. (2015). Solar assisted ground source heat pump in cold climates. Energy Procedia, 82, 623-629.

13. You, T., Wu, W., Shi, W., Wang, B., & Li, X. (2016). An overview of the problems and solutions of soil thermal imbalance of ground-coupled heat pumps in cold regions. Applied Energy, 177, 515-536.
14. Cimmino, M., & Eslami-Nejad, P. (2017). A simulation model for solar assisted shallow ground heat exchangers in series arrangement. Energy and Buildings, 157, 227-246.
15. Mousavi Maleki, S. A., Hizam, H., & Gomes, C. (2017). Estimation of hourly, daily and monthly global solar radiation on inclined surfaces: Models re-visited. Energies, 10(1), 134.
16. Teamah, H. M., & Lightstone, M. F. (2019). Numerical study of the electrical load shift capability of a ground source heat pump system with phase change thermal storage. Energy and Buildings, 199, 235-246.
17. Sommerfeldt, N., & Madani, H. (2019). In-depth techno-economic analysis of PV/Thermal plus ground source heat pump systems for multi-family houses in a heating dominated climate. Solar Energy, 190, 44-62.
18. Trillat-Berdal, V., Souyri, B., & Fraisse, G. (2006). Experimental study of a ground-coupled heat pump combined with thermal solar collectors. Energy and Buildings, 38(12), 1477-1484.
19. Wuestling, M. D., Klein, S. A., & Duffie, J. A. (1985). Promising control alternatives for solar water heating systems.
20. Zhao, Z., Shen, R., Feng, W., Zhang, Y., & Zhang, Y. (2018). Soil thermal balance analysis for a ground source heat pump system in a hot-summer and cold-winter region. Energies, 11(5), 1206.
21. Nam, Y. J., Gao, X. Y., Yoon, S. H., & Lee, K. H. (2015). Study on the performance of a ground source heat pump system assisted by solar thermal storage. Energies, 8(12), 13378-13394.
22. N. R. Canada, "Energy and Greenhouse Gas Emissions (GHGs)," Oct. 06, 2017. https://www.nrcan.gc.ca/energy/facts/energy-ghgs/20063 (accessed Apr. 24, 2020).
23. H. Chen, "G7 Fossil Fuel Subsidy Scorecard," NRDC, 06032018. https://www.nrdc.org/resources/g7-fossil-fuel-subsidy-scorecard (accessed Apr. 24, 2020).
24. N. R. Canada, "Energy Efficiency Trends in Canada 1990 to 2013," Sep. 20, 2016. https://www.nrcan.gc.ca/energy/publications/19030#a3 (accessed Apr.24, 2020)
25. "Drake Landing Solar Community." https://www.dlsc.ca/ (accessed Apr. 24, 2020).
26. "Go Solar- Your guide to harnessing the power of the sun," the City of Vaughan, Vaughan, Ontario, 2009. [Online]. Available: http://www.vaughan.ca/cityhall/environmental_sustainability/General%20Documents/GoSolar_Book-2009.pdf.
27. TRNSYS (v18) – Official Website." http://sel.me.wisc.edu/trnsys/ (accessed Aug. 2020).

28. “Solar Energy Maps Canada (Every Province),” energyhub.org, May 12, 2018. https://energyhub.org/solar-energy-maps-canada/ (accessed Apr. 24, 2020).
29. “Ethylene glycol definition and its feature. https://www.britannica.com/science/ethylene-glycol
30. Hottel, H. C, and Whillier, A., "Evaluation of Flat-Plate Collector Performance," Trans, of Conf. on Use of Solar Energy, Part 1, Vol. 74, University of Arizona Press, 1958.